Title Page

Title:

Loss of *dop-2* causes increased dopamine release and locomotory defects in the presence of ethanol

Running title:

DOP-2 regulates dopamine release in ethanol

Author List:

Pratima Pandey[1,4,5], Anuradha Singh[1,4], Harjot Kaur[3], Anindya Ghosh-Roy[3] and Kavita Babu[1,2,5]

Author Affiliations:

1. Department of Biological Sciences, Indian Institute of Science Education and Research (IISER) Mohali, Knowledge City, Sector 81, SAS Nagar, Manauli PO 140306, Punjab, India.
2. Centre for Neuroscience, Indian Institute of Science, CV Raman Road, Bangalore 560012, Karnataka, India. Co-first authors
3. National Brain Research Centre, Manesar, Nainwal Mode, Gurgaon 122051, Haryana, India.
4. Co-first authors.
5. Corresponding authors: Pratima Pandey (pratima.sharma@babulab.org) and Kavita Babu (kavita.babu@babulab.org or kavitababu@iisc.ac.in).

Keywords: DOP-2, Ethanol, DVA, Neuropeptide and *C. elegans*

Abstract

Ethanol is a widely used drug, excessive consumption of which could lead to medical conditions with diverse symptoms. Ethanol abuse causes disinhibition of memory, attention, speech and locomotion across species. Dopamine signaling plays an essential role in ethanol dependent behaviors in animals ranging from *C. elegans* to humans. We devised an ethanol dependent assay in which mutants in the dopamine autoreceptor, *dop-2,* displayed a unique sedative locomotory behavior causing the animals to move in circles while dragging the posterior half of their body. We identify the posterior dopaminergic sensory neuron as being essential to modulate this behavior. We further demonstrate that in *dop-2* mutants, ethanol exposure increases dopamine secretion and results in enhanced function of the DVA interneuron. DVA releases the neuropeptide NLP-12 and leads to the excitation of cholinergic motor neurons that affect movement. Thus, DOP-2 modulates dopamine levels at the synapse and regulates alcohol induced movement through NLP-12.

Introduction

Alcohol is an easily available abusive drug used world over. Since excessive alcohol intake is detrimental to human health, many studies have focused on understanding the mode of action and dependency of this drug. Behavioral responses to alcohol and susceptibility to alcohol use disorders (AUDs) vary since they are dependent upon environmental, physiological and genetic differences amongst individuals (Prescott and Kendler, 1999; Schuckit and Smith, 1996). Hence, it is still unclear how alcohol functions to modulate various behaviors, making it important to identify and analyze target gene/s and molecular pathways which functions to modulate behavioral phenotype/s upon alcohol intake.

AUDs require functioning through multiple synaptic molecules including acetylcholine (ACh), GABA, glutamate, dopamine (DA), neuropeptide-Y related pathways and ligand gated channels (Reviewed in (Bettinger and Davies, 2014; Harris and Trudell *et al.*, 2008; Spanagel, 2009)). Ethanol (EtOH) intake has been shown to increase DA release which in turn induces the reward pathway and brings about disinhibition of behaviors (reviewed in (Baik, 2013)). The DA pathway comprises of two receptor subfamilies; D1-like (inhibitory) and D2-like (excitatory) receptors that function through the G-protein signaling pathway (Bunzow et al., 1988; Pandey and Harbinder, 2012; Zhou et al., 1990). A special class of D2 autoreceptors have also been identified and are located on dopaminergic neurons, these receptors are thought to regulate the release of DA (reviewed in (Ford, 2014)). In mammals, activation of these receptors lowers the excitability of DA neurons and modulates the release and transmission of dopamine (Beaulieu and Gainetdinov, 2011; Koeltzow et al., 1998; Rivet et al., 1994). Further, the

77 D2 autoreceptors have been associated with alcoholism (Lu et al., 2001; Thanos et al.,
78 2005).

79 *Caenorhabditis elegans* as a model organism is popular for its powerful genetic tools
80 (Corsi et al., 2015) and has been widely utilized for studying the various aspects of
81 neuroactive drugs (Alaimo et al., 2012; Bettinger et al., 2004; Giacomotto and Segalat,
82 2010; Hawkins et al., 2015; Schafer, 2004). *C. elegans* encounters alcohol in its natural
83 habitat (rotten fruits) and hence could be expected to have evolutionarily developed
84 neuronal circuitry allowing for alcohol sensitivity. The DA system is very compact in *C.*
85 *elegans*, with merely eight DA neurons as compared to ~500,000 neurons in the ventral
86 midbrain of humans ((Sulston et al., 1975) and reviewed in (Hegarty et al., 2013)). *C.*
87 *elegans* DA receptors, like their mammalian counterparts also belong to two subfamilies,
88 D1-like and D2-like receptors (Suo et al., 2002, 2003). EtOH shows its effect in a
89 concentration dependent manner, acting as stimulant at lower concentration and
90 depressant at higher concentration. Studies in *C. elegans* have reported that EtOH
91 administration shows dose dependent decline in the locomotor activity with increasing
92 levels of EtOH exposure, which is similar to the depressive effects of EtOH seen in
93 other animal systems (Alaimo et al., 2012; Davies et al., 2003; Hawkins et al., 2015).
94 The internal dose of EtOH responsible for this behavior is similar to that in mammalian
95 systems, indicating that there might exist similar molecular targets (Lee et al., 2009).

96 Utilizing *C. elegans*, we devised an EtOH dependent assay and screened for
97 dopaminergic receptors and pathway mutants. Mutants in the D2-like autoreceptor, *dop-*
98 *2* displayed a novel locomotory phenotype when exposed to 400 mM EtOH. DOP-2 has
99 previously been shown to participate in associative learning and copulation behaviors

(Correa et al., 2015; Voglis and Tavernarakis, 2008). We found that *dop-2* mutant animals slowly dragged their body in concentric circles in what we refer to as Ethanol Induced Sedative (EIS) behavior. Our experiments indicate that *dop-2* mutants show increased dopamine release in the presence of EtOH, which is responsible for the EIS phenotype seen in these animals. Previous work has implicated a circuit through the PDE sensory neurons, the DVA interneuron and cholinergic motor neurons that allow for normal locomotion in *C. elegans* (Bhattacharya et al., 2014; Hu et al., 2011). Our work builds on this previous circuit and goes on to elucidate that the same circuitry is hyperactivated in *dop-2* mutants in the presence of EtOH and this in turn causes the EIS behavior.

Results

Ethanol exposure affects movement in *dop-2* mutants

In *C. elegans,* the DA pathway is widely known to modulate egg laying, defecation, basal slowing, habituation, and associative learning (McDonald et al., 2006; Sawin et al., 2000; Voglis and Tavernarakis, 2008). DA receptors, DOP-1 and DOP-3 function antagonistically to regulate signaling in acetylcholine motor neurons (Allen et al., 2011), while the DA receptor, DOP-2 is expressed presynaptically in all the dopaminergic neurons and has the potential to function as an autoreceptor. However, the *dop-2* mutants do not show any obvious defects that can explain its autoreceptor function. It is possible that under wild-type conditions loss of *dop-2* is compensated for by other regulatory mechanisms in the organism. Modulation of behavior and function through

the dopaminergic system upon exposure to drugs of abuse such as ethanol has been previously established (Kameda et al., 2007; Siciliano et al., 2019). We speculated that exposure of the mutants of the dopaminergic pathway to Ethanol (EtOH) might allow us to screen for possible behavioral defects in these mutants. Previous work has shown that wild type (WT) *C. elegans* show flattening of the body-bends at 400 mM concentration of EtOH (Davies and McIntire, 2004; Davies et al., 2003). We observed a similar phenotype with WT animals, but after a period of 2 hours (h) these animals recovered and began to move in a manner that was similar to WT animals that had not been exposed to EtOH (Fig. 1a-d and Movie 1). We went forward to screen mutants in the dopaminergic pathway for defects in locomotion beyond 2 hours in the presence of 400 mM EtOH and found that mutants in the dopamine autoreceptor, *dop-2*, showed a unique behavior where the *C. elegans* kept moving in circles and compulsively dragged the posterior part of their body (Fig. S1 and Movie 2). During this movement we observed that there was slowing of movement as measured by number of body-bends and a flattening of the body-bends (amplitude of body-bends) that was very pronounced in the posterior half of the animal (Figs. 1e and f). We referred to this behavior as an Ethanol Induced Sedative (EIS) behavior. In order to test if this behavior was seen only in the presence of EtOH or observable in untreated animals as well, we quantified the anterior and posterior body-bends and amplitude of body-bends from untreated WT and *dop-2* mutants and saw no significant difference between both the strains (Fig. 1g and h). We next wanted to test if *dop-2* mutants affect all muscles or largely affect the locomotory body-wall muscle function. To address this question we treated control WT animals, *dop-2* mutants and mutants in the *slo-1* BK Potassium channel that is required

for alcohol sensing (Davies et al., 2003) with EtOH for more than 2 h and counted the number of pharyngeal pumps per minute (min) in each strain. We found that the pharyngeal pumping frequency of *dop-2* mutants was indistinguishable from that of WT animals (Fig. S2). These results suggest that *dop-2* mutants have higher, prolonged locomotory sedative response to EtOH.

The EIS behavior in *dop-2* is modulated through the PDE neuron

Our results suggest that EIS is a *dop-2* dependent behavior. To show that it is indeed dependent on DOP-2 we made transgenic rescue lines with the *Pdop-2*::DOP-2::CFP construct (Correa et al., 2012), and used this line in the EtOH assay and observed that both transgenic rescue lines could completely rescue the *dop-2* mutant phenotype (Figs. 2a and b). We next wanted to identify the neuron through which DOP-2 could be functioning.

There are eight dopaminergic neurons in the *C. elegans* hermaphrodite, two pair of CEP and a pair of ADE neurons in the head and a pair of PDE neurons in the posterior half of the *C. elegans* body (Sulston et al., 1975). All these dopaminergic neurons are mechanosensory in nature and control basal slowing behavior in the animal (Sawin et al., 2000). Our behavioral experiments indicated that the posterior half of the *dop-2* animals was more affected than the anterior in the presence of EtOH. The only dopaminergic neuron with sensory endings at the posterior region is the PDE neuron that is also involved in harsh touch behavior and context dependent modulation of movement (Bhattacharya et al., 2014; Li et al., 2011). Bhattacharya *et al* have recently shown that the PDE neuron through synaptic signaling via the DVA interneuron

regulates the motor circuit in *C. elegans* (Bhattacharya and Francis, 2015; Bhattacharya et al., 2014). From the above information, we hypothesized that the EIS behavior could be due defective dopaminergic signaling from the PDE neuron. Since we were unable to find a PDE specific promoter for rescue experiments, we decided to ablate the PDE sensory neurons in WT and *dop-2* backgrounds and analyzed the PDE ablated animals for ethanol sensitivity (Illustrated in Fig. 2c). We observed that on exposure to EtOH the PDE ablated WT animals displayed no obvious defects in the number of body-bends or amplitude of body-bends when compared to the mock treated animals (Figs. 2d and e). However, upon testing the *dop-2* mutant animals in the EtOH assay we saw that unlike the mock ablated animals that showed the EIS behavior, the *dop-2* mutants with ablated PDE neurons behaved like control animals (Fig. 2d and e). These results indicate that the EIS behavior is DOP-2 dependent and that DOP-2 function in PDE neurons is sufficient to regulate this behavior.

WT animals show EIS behavior in the presence of exogenous dopamine

Our data suggests that DOP-2 is functioning through the DA neuron, PDE and could be dependent on dopamine. D2 like autoreceptors have been shown to modulate the levels of dopamine through the regulation of transporters and components of the dopamine synthesis pathway (reviewed in (Ford, 2014)). However, the function of DOP-2 is still unclear. Since the EIS behavioral model provides us with an experimental system to investigate the function of DOP-2 in sedative movement during exposure to EtOH, hence we examined how DA levels and DA synthesis pathway components might affect the EIS behavior. To address this we utilized the *cat-2* mutants in the EtOH assay. CAT-2 encodes a tyrosine hydroxylase and is required to synthesize DA from tyrosine. The

cat-2 (n4547) mutant used in this study is an allelic deletion and is reported to have 20-30% of WT levels of dopamine (Lints and Emmons, 1999; Sanyal et al., 2004). We performed the EtOH assay with this mutant of *cat-2.* Upon observation and quantitation of *cat-2* mutant behavior it was quite evident that decreased levels of dopamine are not involved in the sedative, sluggish behavior shown by *dop-2* (Figs. 1e, 3a and b). We next generated *cat-2; dop-2* double mutants and performed the EtOH assay with these animals. We observed that this double mutants showed a similar behavior as was seen in *cat-2* mutant animals (Figs. 3a and b). These results indicated that *cat-2* could be functioning upstream of *dop-2* and that the EIS phenotype was unlikely to be caused by decreased dopamine levels.

There are multiple reports indicating the negative regulatory role of the D2 autoreceptor in regulating synaptic levels of dopamine (Benoit-Marand et al., 2001; Rouge-Pont et al., 2002; Schmitz et al., 2002). In order to test if the EIS phenotype was due to increased dopamine levels, we provided WT animals with exogenous dopamine in the EtOH assay. We observed that these animals showed the EIS behavior that was previously observed in *dop-2* mutants. These WT animals treated with exogenous dopamine showed decreased numbers and amplitude of body-bends in the EtOH plate. This phenotype was significantly different when compared to control WT animals treated with either just exogenous DA (no EtOH) or just EtOH (no exogenous DA) (Figs. 3c and d). These results suggest that increased dopamine release is responsible for the EIS behavior in *dop-2* mutant animals.

Mutants in *dop-2* show increased dopamine release in the presence of EtOH

Our results so far have indicated that there could be increased levels of dopamine release in *dop-2* mutants in the presence of EtOH, which is responsible for the EIS behavior in these mutants. To get more insight into the defects in dopamine release in the PDE neurons of *dop-2* mutant animals treated with EtOH, we used FRAP (Fluorescence Recovery After Photobleaching) recordings as a tool to examine DA release (Miesenbock et al., 1998; Samuel et al., 2003). Here we used the previously constructed strain with synaptobrevin-super ecliptic pHluorin reporter fusion (SNB-1::SEpHluorin), which is expressed under the dopaminergic *asic-1* promoter ((Hardaway et al., 2015) and illustrated in Fig. S3). The PDE neuron synapses were examined with pH sensitive GFP (superecliptic pHluorin) attached to a vesicular protein SNB-1. The fluorescence was bleached at the synapses of PDE neuron and the rate of recovery at the bleached area was calculated as a possible measure of DA release. Increased release of dopamine was monitored by the rate of recovery in PDE synapses post bleach. We observed that EtOH exposed *dop-2* mutants showed a significantly faster rate of recovery in the case of *dop-2* mutant animals in presence of EtOH (Figs. 4a and b) and increased rates of fluorescence recovery at 60 s and 120 s time points in *dop-2* animals treated with EtOH (Fig. 4c). We next wanted to test if *dop-2* mutants affect levels of the surface DA transporter DAT-1.

Previous reports indicate that D2 like receptors are involved in the surface localization of DAT-1. We utilized the previously constructed DAT-1::GFP translational fusion line to study DAT-1 expression in *dop-2* mutants (Carvelli et al., 2004). We performed imaging and quantitated the cell surface expression of DAT-1 transporter in PDE neuron in the presence and absence of EtOH in the WT and *dop-2* mutant backgrounds. We

observed a reduction in cell surface expression of DAT-1 in *dop-2* mutants exposed to EtOH (Figs. 4d and e). These experiments indicate that *dop-2* mutants in the presence of EtOH show increased synaptic DA and decreased surface DAT-1.

DAT-1 is present on the DA neurons and recycles DA back into the neuron. We reasoned that if the reuptake mechanism was affected then *dat-1* (DA transporter) deletion mutant should also show EIS like phenotype since DA levels should be higher than WT, but that wasn't the case (Fig. S1). It is possible that loss of *dat-1* is only a part of the phenotype that allows for the EIS behavior in the animals that is seen in *dop-2* mutants treated with EtOH.

DOP-2 functions through DOP-1 present in the DVA neuron

Thus far our data indicates that the EIS behavior seen in *dop-2* animals is modulated by the neurotransmitter DA. PDE has been found to be responsible for the DA effect but how this leads to defects in movement is still unknown. A previous study has elegantly shown that DA released from PDE neurons can activate DOP-1 present on the DVA neuron ((Bhattacharya et al., 2014) and reviewed in (Bhattacharya and Francis, 2015)). The DVA neuron upon activation results in the release of neuropeptide NLP-12 that results in the activation of downstream motor neurons (Hu et al., 2011). The sensory neuron PDE forms strong synaptic connections with the interneuron DVA (Sawin et al., 2000). To understand the circuit through which PDE functions for the EIS phenotype we studied how the deletion of the dopaminergic receptor, *dop-1* could affect the movement in *C. elegans* after EtOH treatment. We found no significant differences in body-bends on comparing *dop-1* mutants with WT animals (Figs. 5a and b). Next we made *dop-2;*

257 *dop-1* double mutants and observed that it showed the same kind of behavior as *dop-1*
258 mutants (Figs. 5a and b). Thus, *dop-1* deletion was able to suppress the EIS phenotype
259 seen in *dop-2* mutants. If deletion of *dop-1* is obstructing DA signaling from PDE to DVA
260 then we reasoned that expressing DOP-1 specifically in DVA would restore the EIS
261 phenotype in the *dop-2; dop-1* double mutant animals. We indeed found that expressing
262 DOP-1 specifically in DVA using the *nlp-12* promoter made the *dop-2; dop-1* animals
263 revert to the *dop-2* like EIS behavior (Figs. 5a and b). These data indicate that EIS is
264 dependent upon DA released from PDE and the DOP-1 receptor present on the DVA
265 neuron.

266 The DVA neuron has been shown previously to function through the neuropeptide NLP-
267 12. NLP-12 release potentially activates the downstream postsynaptic cholinergic motor
268 neurons by binding to its receptors, CKR-2 (cholecystokinin like receptor). Interestingly,
269 it has been shown previously that NLP-12 secretion is directly correlated with the speed
270 of the animal (Hu et al., 2011). We reasoned that increased NLP-12 secretion could
271 allow the animal to show the EIS phenotype. To perform this experiment we
272 overexpressed NLP-12 in the DVA neuron. We found that all three NLP-12
273 overexpression lines showed the EIS behavioral phenotype (Figs. 5c and d). We also
274 tested *nlp-12* mutants and found that they behaved in a manner similar to WT control
275 animals after EtOH treatment (Figs. S4 a and b). We next wanted to test if ablating DVA
276 would affect the EIS behavior in the NLP-12 overexpression line. However, we found
277 that just ablating DVA in WT animals without EtOH treatment caused locomotory
278 defects as has been shown previously ((Li et al., 2006), Figs. S4c and d). Our data so
279 far suggests that dopamine released from PDE signals through DOP-1 receptors in the

DVA interneuron, which in turn releases the neuropeptide NLP-12 in this circuitry is responsible for the EIS behavior in *dop-2* mutants treated with EtOH.

Increased Acetylcholine levels at the NMJ results in EIS behavior

Previous work has shown that DA receptors DOP-1 (D1-like) and DOP-3 (D2-like) regulate locomotion in *C. elegans* (Chase et al., 2004; Omura et al., 2012). Studies also indicate that the hypercontracted state observed in case of ethanol exposure in the animals is due to increased acetylcholine at the NMJ (Hawkins et al., 2015). These studies prompted us to evaluate if dopamine might be involved in regulating locomotion through the cholinergic pathway. Initially we investigated if decreased levels of ACh could display the EIS behavior, but found no significant changes in the locomotion of cholinergic mutants when compared to WT control animals on exposure to EtOH (Fig. S5). We next wanted to test animals with increased ACh release in the presence of EtOH. Previous work has shown that aldicarb treatment causes increased ACh signaling at the NMJ (Hu et al., 2011). Hence, we performed the aldicarb assay followed by treatment of the animals with EtOH. For this experiment, *C. elegans* were exposed to 100 mM aldicarb followed by 400 mM EtOH exposure. We found that WT animals subjected to the above assay showed the EIS phenotype previously seen in *dop-2* mutant animals (Figs. 6a and b). The acetylcholine synthesis pathway mutant *cha-1* was used as a control as it is reported to show resistance to aldicarb (Rand and Russell, 1984). These animals when exposed to aldicarb and EtOH did not show the defect in movement seen in WT *C. elegans* (Figs. 6a and b). As a control *cha-1* mutants were also analyzed with just EtOH (no aldicarb) and these animals also behaved in a manner similar to that of WT control animals (Fig. S5). These experiments indicate that the *dop-*

303 *2* EIS behavior is an outcome of increased cholinergic signaling at the NMJ. ACh
304 signals mainly through the nicotinic ACR-16 receptors present on the postsynaptic
305 body-wall muscle membrane. In *acr-16* mutant there is an 85% decrease in response to
306 ACh when compared to WT animals (Touroutine et al., 2005). To understand the role of
307 the acetylcholine receptors in the EIS behavior, we tested a previously used ACR-
308 16::GFP line for the EIS behavior (Babu et al., 2011). We found that overexpression of
309 ACR-16 caused the animals to show the EIS behavior while mutants in *acr-16* behaved
310 like WT animals after EtOH treatment (Figs. 6c and d). However, the phenotype seen
311 on ACR-16 overexpression was not as robust as that seen with *dop-2* mutant animals.
312 Together these data indicate that elevated muscle excitation through increased
313 acetylcholine is playing a significant role in the EIS behavior of the animal.

314

315 **Discussion**

316 DOP-2 belongs to a family of D2-like inhibitory receptors. It is thought to negatively
317 regulate the release of dopamine by feedback inhibition of dopamine release from
318 presynaptic neurons (Reviewed in (De Mei et al., 2009; Ford, 2014; Mercuri et al.,
319 1997)). In *C. elegans* DOP-2 is only present on the DA neurons making it a very good
320 candidate for autoregulation of DA. However, its deletion does not show defects in DA
321 dependent behaviours as reported for other DA receptors such as DOP-1 and DOP-3
322 (Allen et al., 2011; Chase et al., 2004; Sawin et al., 2000). It is likely that behaviors
323 associated with deletion of neuromodulatory molecules are not easily observable in
324 native conditions since they are required to modulate multiple behaviors and not one

specific behavior (Ford, 2014). EtOH has been shown to increase dopamine release from the mammalian ventral tegmental area and increased dopamine levels were found in the nucleus acccumens (Imperato and Di Chiara, 1986; Weiss et al., 1996; Yim and Gonzales, 2000). Since both loss of D2-like receptors and ethanol (EtOH) tend to increase DA levels, we went on to test *dop-2* deletion mutants for movement defect/s in the presence of EtOH and found a robust behavior involving decrease in body-bends and the flattening of the body-bends which we have termed Ethanol Induced Sedative (EIS) behavior. This behavior was more pronounced in the posterior region of the animal. Although previous studies have reported that *C. elegans* show tolerance towards acute EtOH exposure and after recovery they exhibit various forms of disinhibitions in their behaviors (Mitchell et al., 2010; Topper et al., 2014), our studies describe for the first time the role of chronic EtOH treatment for extended periods of time (400 mM EtOH for upto 24 hrs). Our data also shows that the EIS behavior in *dop-2* mutant animals is due to increased dopamine release.

The synaptic levels of dopamine are maintained by the activities of dopamine transporter (DAT-1), that recycles the dopamine back to the cell in conjunction with the DA autoreceptor (DOP-2) (Benoit-Marand et al., 2000; Schmitz et al., 2002). In mammals the activity of the DA transporter can be controlled by D2-autoreceptors by regulating their surface expression (Benoit-Marand et al., 2011; Cass and Gerhardt, 1994; Dickinson et al., 1999; Mayfield and Zahniser, 2001; Schmitz et al., 2002; Wu et al., 2002). This occurs at least partially via an increase in DAT cell surface expression after D2-receptor activation (Mayfield and Zahniser, 2001). However, D2-antagonists or D2 deletion could not alter DAT dependent DA uptake (Anzalone et al., 2012;

348 Beckstead and Williams, 2007; Bello et al., 2011; Benoit-Marand et al., 2011; Benoit-
349 Marand et al., 2001; Kennedy et al., 1992). Our FRAP experiments conducted in the
350 presence of increased EtOH showed increased release of DA and in the absence of
351 *dop-2*. Further the membrane expression of DAT-1 was decreased in EtOH treated *dop-*
352 *2* mutant animals when compared to control animals. Hence we show that DAT-1
353 surface transport is dependent upon DOP-2. However, since loss of *dat-1* does not
354 show the EIS phenotype, it is likely that multiple factors including increased dopamine
355 release contribute to the EIS behavior and it is not dependent on just loss of DAT-1
356 membrane expression.

357 All our data points towards the fact that the posterior region of the animal is more
358 affected then the anterior region during EIS behavior in *dop-2* mutants. Neuronal
359 ablation experiments demonstrate that the posterior DA neuron, PDE is responsible for
360 the *dop-2* EIS phenotype. The PDE neuron forms multiple unidirectional synapses with
361 the DVA interneuron. Our experiments implicate PDE function through the DVA neuron
362 to allow for changes in downstream motor circuitry. These findings are in line with work
363 that has previously reported that the PDE neuron makes direct synaptic contacts with
364 the DVA neuron (Bhattacharya et al., 2014). DVA is known to modulate locomotion both
365 positively and negatively by providing a unique mechanism whereby a single neuron
366 can fine-tune motor activity (Li et al., 2006). The DVA interneuron has connections with
367 both motor neurons and interneurons and relays information for normal locomotion
368 (Bhattacharya et al., 2014; Gray et al., 2005). One mechanism of maintaining normal
369 locomotion especially in conditions of stress like EtOH exposure could involve
370 dopamine release from PDE regulating the movement of *C. elegans* through DVA. Our

work further implicates the role of the DOP-1 receptor in DVA and the requirement of this pathway to maintain the EIS behavior seen in *dop-2* mutants. The DVA neuron expresses the DA receptor DOP-1, a D1-like excitatory receptor (Bhattacharya et al., 2014). Further, in *Drosophila* and mammals it has been demonstrated that D1-like DA receptors promote EtOH-induced disinhibition (Abrahao et al., 2011; Kong et al., 2010).

A prior study has shown that movement induces NLP-12 release from DVA neurons and enhances ACh release at NMJs (Hu et al., 2011). Further, multiple studies have demonstrated that neuropeptides modulate neuronal activity and synaptic transmission (Bhardwaj et al., 2018; Edwards et al., 2009; Hu et al., 2011; Jacob and Kaplan, 2003; Kass et al., 2001; Sieburth et al., 2007; Speese et al., 2007; Sumakovic et al., 2009). In this study we show that overexpressing just the NLP-12 neuropeptide in the DVA interneuron is sufficient to mimic the EIS phenotype seen in *dop-2* mutants, again implicating neuropeptides in synaptic functions.

Previous work that has shown that in *Drosophila melanogaster*, mutants in a gene called *arouser* cause the animal to show increased sedation in the presence of EtOH as well as show increased boutons at the NMJ, indicating a link between increased neuromuscular signaling and greater susceptibility to alcohol (Eddison et al., 2011). Our data demonstrates that the EIS behavior seen in *dop-2* mutants could occur because of changes in neurotransmission at the *C. elegans* NMJ. We also show that increased neurotransmission brought about by the drug aldicarb or overexpressing acetycholine receptors at the body-wall muscle both cause EIS behavior in *C. elegans*.

Overall our data implicates *dop-2* in the ethanol induced sedative phenotype by showing that 1. Mutants in *dop-2* show increased dopamine release in the PDE neuron upon chronic ethanol treatment. 2. The increased dopamine released from the PDE sensory neuron causes increased release of the neuropeptide, NLP-12 from the DVA interneuron. 3. Increased NLP-12 release could cause increased cholinergic neuronal function and result in the EIS phenotype observed. This circuit is illustrated in Fig. 7.

Taken in its entirety, our work along with previous work paves a path for using *C. elegans* as a model system to study the molecular players involved in alcohol dependent locomotory functions (Davies et al., 2003; Mitchell et al., 2007).

Methods:

Strains

Animals were maintained according to standard protocols (Brenner, 1974). N2 Bristol was used as the wild type (WT) strain. The mutant strains used in this study were; *dop-2(vs105), dop-3(vs106), dop-1(vs100), cat-2(n4547), cha-1(p1152), acr-16(ok789), slo-1(eg142), dat-1(ok157)* and *nlp-12(ok335)*.

Constructs and transgenes

All constructs were generated using *pPD95.75* as the backbone with standard restriction digestion cloning procedures (Russell, 2001). Transgenic lines were generated by microinjection of the desired plasmid as previously described (Mello and Fire, 1995). The *Pdop-2*::DOP-2::mCherry construct was obtained from Rene Garcia

Lab (Correa et al., 2012). The *nlp-12* promoter used in pBAB911 was cloned by amplifying a 355 bp upstream region of the *nlp-12* gene from genomic DNA using AACTGCAGGGCCGAGACGAATCCGGAGG (AS1) and CGGGATCCGCATTTTGTCGGAGGCAATT (AS4) primers and cloned into the *pPD95.75* vector using Pst I and Bam HI sites. The pBAB913 construct was generated by cloning P*nlp-12* into a previously made P*exp-1*::*sl2*::wrmScarlet vector using Pst I and Xma I sites that removed P*exp-1*. The pBAB912 construct contains a 1.7 kb genomic region of *nlp-12* amplified from genomic DNA using AACTGCAGGGCCGAGACGAATCCGGAGG (AS1) and CGGGATCCGAAAATGTGTCGCTTCGAGAC (AS3) primers. The PCR amplified fragment was cloned into the *pPD95.75* vector using Pst I and Bam HI sites, for generating the *nlp-12* overexpression lines. For *dop-1* rescue experiment *dop-1* cDNA (1.2kb) was cloned under the *nlp-12* promoter in pBAB913 using Xma I and Kpn I sites.

A complete list of strains, primers and plasmids used in this study are available in the supplementary tables S1, S2 and S3 respectively.

Ethanol induced behavioral assay

C. elegans were synchronized by bleaching and grown on nematode growth media (NGM) plates. They were maintained in well-fed conditions till the assay. The Ethanol (EtOH) plates were prepared using unseeded plates i.e. without food plates that were dried for 3 hours (h) under airflow in the biosafety cabinet. This was followed by spreading EtOH (400 mM) on the plates. The plates were then sealed with parafilm and were allowed to equilibrate for 2 h at 20^{o}C. Adult animals were initially transferred to unseeded plates for 15 to 20 seconds (sec) and then moved to the EtOH plates. 10

436 animals were used for each set and the experiment was done in triplicate for every
437 genotype tested. All animals initially showed coiling behavior and paralyzed within 10
438 minutes (min) of EtOH exposure as has been previously reported (Davies et al., 2003).
439 Recovery of *C. elegans* started in all the strains except *dop-2* in approximately 30 min.
440 All the strains used for assays including WT showed Ethanol Induced Sedentary (EIS) -
441 like behavior at around 30 min when movement started. However, most strains regained
442 their normal locomotory behavior after more then 60 min. The plates were incubated
443 overnight (16- 20 h) to visualize the tracks. The quantitative analysis of behavior was
444 done at 120 min for all the strains by recording the videos10 frames/sec for 1 min on the
445 AxioCam MRm (Carl Zeiss) using the micromanager software. The anterior and
446 posterior body-bends and amplitude of body-bends were quantified separately for each
447 animal using the imageJ software (Schindelin et al., 2012), n=30 animals were observed
448 for each genotype for body-bends and n=20 for the amplitude of body-bends. Videos
449 obtained from the same animal were used to quantify both body-bends and amplitude of
450 locomotion. The results were plotted as graphs using GraphPad Prism v6 and statistics
451 were evaluated using one-way ANOVA.

452 **Exogenous Dopamine Assay**

453 For exogenous dopamine application, 1 M freshly prepared dopamine was used as
454 previously described (Baidya et al., 2014). The final concentration of dopamine used
455 was 40 mM. Dopamine was spread on EtOH plates for EtOH + dopamine experiments
456 and on unseeded dry plates for only dopamine exposure experiments. The plates were
457 protected from light and used within 10 min of preparation for each assay. Animals were

458 transferred from unseeded plates to the assay plate and their behavior was analyzed by
459 making 1 min videos at 10 frames/sec after 2 h of dopamine/EtOH exposure.

460 **Aldicarb treatment prior to the EtOH assay**

461 This assay was modified from the aldicarb assay to study the behavior of *C. elegans* on
462 EtOH exposure after aldicarb treatment. The aldicarb assay was performed as
463 described previously (Mahoney et al., 2006; Sieburth et al., 2005; Vashlishan et al.,
464 2008). Briefly, plates with 1 mM aldicarb (Sigma- Aldrich 33386) were prepared 1 day
465 prior to the assay and dried. *C. elegans* were transferred to aldicarb plates for 60 min
466 and then moved to EtOH plates after which they were analyzed as previously described
467 in the EtOH induced behavioral assay section.

468 **Microscopy**

469 The DAT-1::GFP imaging experiment was performed on the Leica SP8 confocal
470 microscope using the Argon laser at 10% gain. Young adult animals were immobilized
471 using 30 mg/ml BDM (2,3-ButaneDione monoxime) on 2% agarose. All the image
472 quantitation was done taking whole cell body expression of GFP using FIJI.
473 Experiments were performed both with and without EtOH exposure.

474 **Neuronal ablation**

475 The ablation of PDE and DVA neurons were done using Bruker Corporations ULTIMA
476 two photon IR laser system. In which, one laser was used for imaging (920nm for GFP,
477 1040nm for mScarlet) and another laser for ablating the neurons (720 nm, irradiation
478 duration-20ms, pulse width 80fs, power~23mW) as described in (Basu et al., 2017).
479 During ablation, L2 staged worms were immobilized on 5% agarose pads using 10mM

480 levamisole hydrochloride (Sigma-Aldrich 10380000) or 0.1 μm-diameter polystyrene
481 beads (00876-15; Polystyrene suspension). These worms were then recovered using
482 mouth pipette onto the newly seeded NGM plates and were allowed to grow uptill young
483 adult stage. The worms were then evaluated in the EtOH induced behavioral assay.

484 **FRAP experiments**

485 The increased extracellular release kinematics of dopamine in the presence of EtOH
486 based on DA vesicle fusion, was analyzed and observed using the dopaminergic
487 promoter (P*asic-1*) tagged with pH sensitive synaptobrevin-super ecliptic pHluorin
488 reporter fusion construct (SNB-1::SEpHluorin) (Hardaway et al., 2015; Samuel et al.,
489 2003; Voglis and Tavernarakis, 2008). Young adult animals were mounted on 2%
490 agarose pads and paralyzed using 0.05% levamisole hydrochloride (Sigma-Aldrich
491 10380000). FRAP experiments were performed on the Leica SP8 inverted confocal
492 microscope. PDE synapses were identified by Synaptobrevin::SEpHluorin fluorescence.
493 Bleaching was done using the 488 nm argon laser, 80% bleach power for 5-10 sec to
494 an intensity of 10-15% of original fluorescence value. Fluorescence was monitored
495 every 10 sec for 2 min and analyzed using FIJI software. The percentage recovery was
496 calculated at each time point and 20 synapses were analyzed per genotype. The data
497 was plotted using GraphPad Prism v6 and analyzed using non-linear regression plotting
498 and one phase association exponential equation was used to analyze this data.

499 **Statistical analysis**

500 All statistical analyses were performed by using GraphPad Prism Version 6.0. The error
501 bars represent SEM. Statistical comparisons were done using one-way ANOVA with

Turkey-Kramer multiple comparison test. The level of significance was set as "*" indicates $p < 0.05$, "**" indicates $p < 0.01$ and "***" indicates $p < 0.001$.

References

Abrahao, K.P., Quadros, I.M., and Souza-Formigoni, M.L. (2011). Nucleus accumbens dopamine D(1) receptors regulate the expression of ethanol-induced behavioural sensitization. Int J Neuropsychopharmacol *14*, 175-185.

Alaimo, J.T., Davis, S.J., Song, S.S., Burnette, C.R., Grotewiel, M., Shelton, K.L., Pierce-Shimomura, J.T., Davies, A.G., and Bettinger, J.C. (2012). Ethanol metabolism and osmolarity modify behavioral responses to ethanol in C. elegans. Alcohol Clin Exp Res *36*, 1840-1850.

Allen, A.T., Maher, K.N., Wani, K.A., Betts, K.E., and Chase, D.L. (2011). Coexpressed D1- and D2-like dopamine receptors antagonistically modulate acetylcholine release in Caenorhabditis elegans. Genetics *188*, 579-590.

Anzalone, A., Lizardi-Ortiz, J.E., Ramos, M., De Mei, C., Hopf, F.W., Iaccarino, C., Halbout, B., Jacobsen, J., Kinoshita, C., Welter, M.*, et al.* (2012). Dual control of dopamine synthesis and release by presynaptic and postsynaptic dopamine D2 receptors. The Journal of neuroscience : the official journal of the Society for Neuroscience *32*, 9023-9034.

Babu, K., Hu, Z., Chien, S.C., Garriga, G., and Kaplan, J.M. (2011). The immunoglobulin super family protein RIG-3 prevents synaptic potentiation and regulates Wnt signaling. Neuron *71*, 103-116.

Baidya, M., Genovez, M., Torres, M., and Chao, M.Y. (2014). Dopamine modulation of avoidance behavior in Caenorhabditis elegans requires the NMDA receptor NMR-1. PloS one *9*, e102958.

Baik, J.H. (2013). Dopamine signaling in reward-related behaviors. Front Neural Circuits *7*, 152.

Basu, A., Dey, S., Puri, D., Das Saha, N., Sabharwal, V., Thyagarajan, P., Srivastava, P., Koushika, S.P., and Ghosh-Roy, A. (2017). let-7 miRNA controls CED-7 homotypic adhesion and EFF-1-mediated axonal self-fusion to restore touch sensation following injury. Proceedings of the National Academy of Sciences of the United States of America *114*, E10206-E10215.

Beaulieu, J.M., and Gainetdinov, R.R. (2011). The physiology, signaling, and pharmacology of dopamine receptors. Pharmacol Rev *63*, 182-217.

Beckstead, M.J., and Williams, J.T. (2007). Long-term depression of a dopamine IPSC. The Journal of neuroscience : the official journal of the Society for Neuroscience *27*, 2074-2080.

Bello, E.P., Mateo, Y., Gelman, D.M., Noain, D., Shin, J.H., Low, M.J., Alvarez, V.A., Lovinger, D.M., and Rubinstein, M. (2011). Cocaine supersensitivity and enhanced motivation for reward in mice lacking dopamine D2 autoreceptors. Nat Neurosci *14*, 1033-1038.

Benoit-Marand, M., Ballion, B., Borrelli, E., Boraud, T., and Gonon, F. (2011). Inhibition of dopamine uptake by D2 antagonists: an in vivo study. J Neurochem *116*, 449-458.

Benoit-Marand, M., Borrelli, E., and Gonon, F. (2001). Inhibition of dopamine release via presynaptic D2 receptors: time course and functional characteristics in vivo. The Journal of neuroscience : the official journal of the Society for Neuroscience *21*, 9134-9141.

564 Benoit-Marand, M., Jaber, M., and Gonon, F. (2000). Release and elimination of
565 dopamine in vivo in mice lacking the dopamine transporter: functional consequences.
566 Eur J Neurosci *12*, 2985-2992.
567 Bettinger, J.C., Carnell, L., Davies, A.G., and McIntire, S.L. (2004). The use of
568 Caenorhabditis elegans in molecular neuropharmacology. Int Rev Neurobiol *62*, 195-
569 212.
570 Bhardwaj, A., Thapliyal, S., Dahiya, Y., and Babu, K. (2018). FLP-18 Functions through
571 the G-Protein-Coupled Receptors NPR-1 and NPR-4 to Modulate Reversal Length in
572 Caenorhabditis elegans. The Journal of neuroscience : the official journal of the Society
573 for Neuroscience *38*, 4641-4654.
574 Bhattacharya, R., and Francis, M.M. (2015). In the proper context: Neuropeptide
575 regulation of behavioral transitions during food searching. Worm *4*, e1062971.
576 Bhattacharya, R., Touroutine, D., Barbagallo, B., Climer, J., Lambert, C.M., Clark, C.M.,
577 Alkema, M.J., and Francis, M.M. (2014). A conserved dopamine-cholecystokinin
578 signaling pathway shapes context-dependent Caenorhabditis elegans behavior. PLoS
579 genetics *10*, e1004584.
580 Brenner, S. (1974). The genetics of Caenorhabditis elegans. Genetics *77*, 71-94.
581 Bunzow, J.R., Van Tol, H.H., Grandy, D.K., Albert, P., Salon, J., Christie, M., Machida,
582 C.A., Neve, K.A., and Civelli, O. (1988). Cloning and expression of a rat D2 dopamine
583 receptor cDNA. Nature *336*, 783-787.
584 Carvelli, L., McDonald, P.W., Blakely, R.D., and DeFelice, L.J. (2004). Dopamine
585 transporters depolarize neurons by a channel mechanism. Proceedings of the National
586 Academy of Sciences of the United States of America *101*, 16046-16051.
587 Cass, W.A., and Gerhardt, G.A. (1994). Direct in vivo evidence that D2 dopamine
588 receptors can modulate dopamine uptake. Neurosci Lett *176*, 259-263.
589 Chase, D.L., Pepper, J.S., and Koelle, M.R. (2004). Mechanism of extrasynaptic
590 dopamine signaling in Caenorhabditis elegans. Nat Neurosci *7*, 1096-1103.
591 Correa, P., LeBoeuf, B., and Garcia, L.R. (2012). C. elegans dopaminergic D2-like
592 receptors delimit recurrent cholinergic-mediated motor programs during a goal-oriented
593 behavior. PLoS genetics *8*, e1003015.
594 Correa, P.A., Gruninger, T., and Garcia, L.R. (2015). DOP-2 D2-Like Receptor
595 Regulates UNC-7 Innexins to Attenuate Recurrent Sensory Motor Neurons during C.
596 elegans Copulation. The Journal of neuroscience : the official journal of the Society for
597 Neuroscience *35*, 9990-10004.
598 Corsi, A.K., Wightman, B., and Chalfie, M. (2015). A Transparent Window into Biology:
599 A Primer on Caenorhabditis elegans. Genetics *200*, 387-407.
600 Davies, A.G., and McIntire, S.L. (2004). Using C. elegans to screen for targets of
601 ethanol and behavior-altering drugs. Biol Proced Online *6*, 113-119.
602 Davies, A.G., Pierce-Shimomura, J.T., Kim, H., VanHoven, M.K., Thiele, T.R., Bonci, A.,
603 Bargmann, C.I., and McIntire, S.L. (2003). A central role of the BK potassium channel in
604 behavioral responses to ethanol in C. elegans. Cell *115*, 655-666.
605 De Mei, C., Ramos, M., Iitaka, C., and Borrelli, E. (2009). Getting specialized:
606 presynaptic and postsynaptic dopamine D2 receptors. Curr Opin Pharmacol *9*, 53-58.
607 Dickinson, S.D., Sabeti, J., Larson, G.A., Giardina, K., Rubinstein, M., Kelly, M.A.,
608 Grandy, D.K., Low, M.J., Gerhardt, G.A., and Zahniser, N.R. (1999). Dopamine D2

receptor-deficient mice exhibit decreased dopamine transporter function but no changes in dopamine release in dorsal striatum. J Neurochem *72*, 148-156.

Eddison, M., Guarnieri, D.J., Cheng, L., Liu, C.H., Moffat, K.G., Davis, G., and Heberlein, U. (2011). arouser reveals a role for synapse number in the regulation of ethanol sensitivity. Neuron *70*, 979-990.

Edwards, S.L., Charlie, N.K., Richmond, J.E., Hegermann, J., Eimer, S., and Miller, K.G. (2009). Impaired dense core vesicle maturation in Caenorhabditis elegans mutants lacking Rab2. J Cell Biol *186*, 881-895.

Ford, C.P. (2014). The role of D2-autoreceptors in regulating dopamine neuron activity and transmission. Neuroscience *282*, 13-22.

Giacomotto, J., and Segalat, L. (2010). High-throughput screening and small animal models, where are we? Br J Pharmacol *160*, 204-216.

Gray, J.M., Hill, J.J., and Bargmann, C.I. (2005). A circuit for navigation in Caenorhabditis elegans. Proceedings of the National Academy of Sciences of the United States of America *102*, 3184-3191.

Hardaway, J.A., Sturgeon, S.M., Snarrenberg, C.L., Li, Z., Xu, X.Z., Bermingham, D.P., Odiase, P., Spencer, W.C., Miller, D.M., 3rd, Carvelli, L.*, et al.* (2015). Glial Expression of the Caenorhabditis elegans Gene swip-10 Supports Glutamate Dependent Control of Extrasynaptic Dopamine Signaling. The Journal of neuroscience : the official journal of the Society for Neuroscience *35*, 9409-9423.

Hawkins, E.G., Martin, I., Kondo, L.M., Judy, M.E., Brings, V.E., Chan, C.L., Blackwell, G.G., Bettinger, J.C., and Davies, A.G. (2015). A novel cholinergic action of alcohol and the development of tolerance to that effect in Caenorhabditis elegans. Genetics *199*, 135-149.

Hegarty, S.V., Sullivan, A.M., and O'Keeffe, G.W. (2013). Midbrain dopaminergic neurons: a review of the molecular circuitry that regulates their development. Developmental biology *379*, 123-138.

Hu, Z., Pym, E.C., Babu, K., Vashlishan Murray, A.B., and Kaplan, J.M. (2011). A neuropeptide-mediated stretch response links muscle contraction to changes in neurotransmitter release. Neuron *71*, 92-102.

Imperato, A., and Di Chiara, G. (1986). Preferential stimulation of dopamine release in the nucleus accumbens of freely moving rats by ethanol. J Pharmacol Exp Ther *239*, 219-228.

Jacob, T.C., and Kaplan, J.M. (2003). The EGL-21 carboxypeptidase E facilitates acetylcholine release at Caenorhabditis elegans neuromuscular junctions. The Journal of neuroscience : the official journal of the Society for Neuroscience *23*, 2122-2130.

Kameda, S.R., Frussa-Filho, R., Carvalho, R.C., Takatsu-Coleman, A.L., Ricardo, V.P., Patti, C.L., Calzavara, M.B., Lopez, G.B., Araujo, N.P., Abilio, V.C.*, et al.* (2007). Dissociation of the effects of ethanol on memory, anxiety, and motor behavior in mice tested in the plus-maze discriminative avoidance task. Psychopharmacology (Berl) *192*, 39-48.

Kass, J., Jacob, T.C., Kim, P., and Kaplan, J.M. (2001). The EGL-3 proprotein convertase regulates mechanosensory responses of Caenorhabditis elegans. The Journal of neuroscience : the official journal of the Society for Neuroscience *21*, 9265-9272.

Kennedy, R.T., Jones, S.R., and Wightman, R.M. (1992). Dynamic observation of dopamine autoreceptor effects in rat striatal slices. J Neurochem *59*, 449-455.
Koeltzow, T.E., Xu, M., Cooper, D.C., Hu, X.T., Tonegawa, S., Wolf, M.E., and White, F.J. (1998). Alterations in dopamine release but not dopamine autoreceptor function in dopamine D3 receptor mutant mice. The Journal of neuroscience : the official journal of the Society for Neuroscience *18*, 2231-2238.
Kong, E.C., Woo, K., Li, H., Lebestky, T., Mayer, N., Sniffen, M.R., Heberlein, U., Bainton, R.J., Hirsh, J., and Wolf, F.W. (2010). A pair of dopamine neurons target the D1-like dopamine receptor DopR in the central complex to promote ethanol-stimulated locomotion in Drosophila. PloS one *5*, e9954.
Lee, J., Jee, C., and McIntire, S.L. (2009). Ethanol preference in C. elegans. Genes Brain Behav *8*, 578-585.
Li, W., Feng, Z., Sternberg, P.W., and Xu, X.Z. (2006). A C. elegans stretch receptor neuron revealed by a mechanosensitive TRP channel homologue. Nature *440*, 684-687.
Li, W., Kang, L., Piggott, B.J., Feng, Z., and Xu, X.Z. (2011). The neural circuits and sensory channels mediating harsh touch sensation in Caenorhabditis elegans. Nat Commun *2*, 315.
Lints, R., and Emmons, S.W. (1999). Patterning of dopaminergic neurotransmitter identity among Caenorhabditis elegans ray sensory neurons by a TGFbeta family signaling pathway and a Hox gene. Development *126*, 5819-5831.
Lu, R.B., Lee, J.F., Ko, H.C., and Lin, W.W. (2001). Dopamine D2 receptor gene (DRD2) is associated with alcoholism with conduct disorder. Alcohol Clin Exp Res *25*, 177-184.
Mahoney, T.R., Luo, S., and Nonet, M.L. (2006). Analysis of synaptic transmission in Caenorhabditis elegans using an aldicarb-sensitivity assay. Nat Protoc *1*, 1772-1777.
Mayfield, R.D., and Zahniser, N.R. (2001). Dopamine D2 receptor regulation of the dopamine transporter expressed in Xenopus laevis oocytes is voltage-independent. Mol Pharmacol *59*, 113-121.
McDonald, P.W., Jessen, T., Field, J.R., and Blakely, R.D. (2006). Dopamine signaling architecture in Caenorhabditis elegans. Cell Mol Neurobiol *26*, 593-618.
Mello, C., and Fire, A. (1995). DNA transformation. Methods in cell biology *48*, 451-482.
Mercuri, N.B., Saiardi, A., Bonci, A., Picetti, R., Calabresi, P., Bernardi, G., and Borrelli, E. (1997). Loss of autoreceptor function in dopaminergic neurons from dopamine D2 receptor deficient mice. Neuroscience *79*, 323-327.
Miesenbock, G., De Angelis, D.A., and Rothman, J.E. (1998). Visualizing secretion and synaptic transmission with pH-sensitive green fluorescent proteins. Nature *394*, 192-195.
Mitchell, P., Mould, R., Dillon, J., Glautier, S., Andrianakis, I., James, C., Pugh, A., Holden-Dye, L., and O'Connor, V. (2010). A differential role for neuropeptides in acute and chronic adaptive responses to alcohol: behavioural and genetic analysis in Caenorhabditis elegans. PloS one *5*, e10422.
Mitchell, P.H., Bull, K., Glautier, S., Hopper, N.A., Holden-Dye, L., and O'Connor, V. (2007). The concentration-dependent effects of ethanol on Caenorhabditis elegans behaviour. Pharmacogenomics J *7*, 411-417.
Omura, D.T., Clark, D.A., Samuel, A.D., and Horvitz, H.R. (2012). Dopamine signaling is essential for precise rates of locomotion by C. elegans. PloS one *7*, e38649.

699 Pandey, P., and Harbinder, S. (2012). The Caenorhabditis elegans D2-like dopamine
700 receptor DOP-2 physically interacts with GPA-14, a Galphai subunit. J Mol Signal *7*, 3.
701 Rand, J.B., and Russell, R.L. (1984). Choline acetyltransferase-deficient mutants of the
702 nematode Caenorhabditis elegans. Genetics *106*, 227-248.
703 Rivet, J.M., Audinot, V., Gobert, A., Peglion, J.L., and Millan, M.J. (1994). Modulation of
704 mesolimbic dopamine release by the selective dopamine D3 receptor antagonist, (+)-S
705 14297. Eur J Pharmacol *265*, 175-177.
706 Rouge-Pont, F., Usiello, A., Benoit-Marand, M., Gonon, F., Piazza, P.V., and Borrelli, E.
707 (2002). Changes in extracellular dopamine induced by morphine and cocaine: crucial
708 control by D2 receptors. The Journal of neuroscience : the official journal of the Society
709 for Neuroscience *22*, 3293-3301.
710 Russell, J.S.a.D. (2001). Molecular Cloning: A Laboratory Manual.
711 Samuel, A.D., Silva, R.A., and Murthy, V.N. (2003). Synaptic activity of the AFD neuron
712 in Caenorhabditis elegans correlates with thermotactic memory. The Journal of
713 neuroscience : the official journal of the Society for Neuroscience *23*, 373-376.
714 Sanyal, S., Wintle, R.F., Kindt, K.S., Nuttley, W.M., Arvan, R., Fitzmaurice, P., Bigras,
715 E., Merz, D.C., Hebert, T.E., van der Kooy, D.*, et al.* (2004). Dopamine modulates the
716 plasticity of mechanosensory responses in Caenorhabditis elegans. The EMBO journal
717 *23*, 473-482.
718 Sawin, E.R., Ranganathan, R., and Horvitz, H.R. (2000). C. elegans locomotory rate is
719 modulated by the environment through a dopaminergic pathway and by experience
720 through a serotonergic pathway. Neuron *26*, 619-631.
721 Schafer, W.R. (2004). Addiction research in a simple animal model: the nematode
722 Caenorhabditis elegans. Neuropharmacology *47 Suppl 1*, 123-131.
723 Schindelin, J., Arganda-Carreras, I., Frise, E., Kaynig, V., Longair, M., Pietzsch, T.,
724 Preibisch, S., Rueden, C., Saalfeld, S., Schmid, B.*, et al.* (2012). Fiji: an open-source
725 platform for biological-image analysis. Nature methods *9*, 676-682.
726 Schmitz, Y., Schmauss, C., and Sulzer, D. (2002). Altered dopamine release and
727 uptake kinetics in mice lacking D2 receptors. The Journal of neuroscience : the official
728 journal of the Society for Neuroscience *22*, 8002-8009.
729 Siciliano, C.A., Mauterer, M.I., Fordahl, S.C., and Jones, S.R. (2019). Modulation of
730 striatal dopamine dynamics by cocaine self-administration and amphetamine treatment
731 in female rats. Eur J Neurosci.
732 Sieburth, D., Ch'ng, Q., Dybbs, M., Tavazoie, M., Kennedy, S., Wang, D., Dupuy, D.,
733 Rual, J.F., Hill, D.E., Vidal, M.*, et al.* (2005). Systematic analysis of genes required for
734 synapse structure and function. Nature *436*, 510-517.
735 Sieburth, D., Madison, J.M., and Kaplan, J.M. (2007). PKC-1 regulates secretion of
736 neuropeptides. Nat Neurosci *10*, 49-57.
737 Speese, S., Petrie, M., Schuske, K., Ailion, M., Ann, K., Iwasaki, K., Jorgensen, E.M.,
738 and Martin, T.F. (2007). UNC-31 (CAPS) is required for dense-core vesicle but not
739 synaptic vesicle exocytosis in Caenorhabditis elegans. The Journal of neuroscience :
740 the official journal of the Society for Neuroscience *27*, 6150-6162.
741 Sulston, J., Dew, M., and Brenner, S. (1975). Dopaminergic neurons in the nematode
742 Caenorhabditis elegans. J Comp Neurol *163*, 215-226.
743 Sumakovic, M., Hegermann, J., Luo, L., Husson, S.J., Schwarze, K., Olendrowitz, C.,
744 Schoofs, L., Richmond, J., and Eimer, S. (2009). UNC-108/RAB-2 and its effector RIC-

19 are involved in dense core vesicle maturation in Caenorhabditis elegans. J Cell Biol *186*, 897-914.

Suo, S., Sasagawa, N., and Ishiura, S. (2002). Identification of a dopamine receptor from Caenorhabditis elegans. Neurosci Lett *319*, 13-16.

Suo, S., Sasagawa, N., and Ishiura, S. (2003). Cloning and characterization of a Caenorhabditis elegans D2-like dopamine receptor. J Neurochem *86*, 869-878.

Thanos, P.K., Rivera, S.N., Weaver, K., Grandy, D.K., Rubinstein, M., Umegaki, H., Wang, G.J., Hitzemann, R., and Volkow, N.D. (2005). Dopamine D2R DNA transfer in dopamine D2 receptor-deficient mice: effects on ethanol drinking. Life Sci *77*, 130-139.

Topper, S.M., Aguilar, S.C., Topper, V.Y., Elbel, E., and Pierce-Shimomura, J.T. (2014). Alcohol disinhibition of behaviors in C. elegans. PloS one *9*, e92965.

Touroutine, D., Fox, R.M., Von Stetina, S.E., Burdina, A., Miller, D.M., 3rd, and Richmond, J.E. (2005). acr-16 encodes an essential subunit of the levamisole-resistant nicotinic receptor at the Caenorhabditis elegans neuromuscular junction. The Journal of biological chemistry *280*, 27013-27021.

Vashlishan, A.B., Madison, J.M., Dybbs, M., Bai, J., Sieburth, D., Ch'ng, Q., Tavazoie, M., and Kaplan, J.M. (2008). An RNAi screen identifies genes that regulate GABA synapses. Neuron *58*, 346-361.

Voglis, G., and Tavernarakis, N. (2008). A synaptic DEG/ENaC ion channel mediates learning in C. elegans by facilitating dopamine signalling. The EMBO journal *27*, 3288-3299.

Weiss, F., Parsons, L.H., Schulteis, G., Hyytia, P., Lorang, M.T., Bloom, F.E., and Koob, G.F. (1996). Ethanol self-administration restores withdrawal-associated deficiencies in accumbal dopamine and 5-hydroxytryptamine release in dependent rats. The Journal of neuroscience : the official journal of the Society for Neuroscience *16*, 3474-3485.

Wu, Q., Reith, M.E., Walker, Q.D., Kuhn, C.M., Carroll, F.I., and Garris, P.A. (2002). Concurrent autoreceptor-mediated control of dopamine release and uptake during neurotransmission: an in vivo voltammetric study. The Journal of neuroscience : the official journal of the Society for Neuroscience *22*, 6272-6281.

Yim, H.J., and Gonzales, R.A. (2000). Ethanol-induced increases in dopamine extracellular concentration in rat nucleus accumbens are accounted for by increased release and not uptake inhibition. Alcohol *22*, 107-115.

Zhou, Q.Y., Grandy, D.K., Thambi, L., Kushner, J.A., Van Tol, H.H., Cone, R., Pribnow, D., Salon, J., Bunzow, J.R., and Civelli, O. (1990). Cloning and expression of human and rat D1 dopamine receptors. Nature *347*, 76-80.

Acknowledgments

The authors are especially grateful to Yogesh Dahiya for help with the FRAP experiment. We thank Randy Blakely, Rene Garcia and Ron Evans for reagents. A number of strains were provided by CGC, which is funded by NIH Office of Research Infrastructure Programs (P40 OD010440). The authors thank Ankit Negi for routine help and the IISER Mohali Confocal facility for use of the confocal microscope.

AS thanks Council of Scientific and Industrial Research (CSIR)- University Grants Commision (UGC) for a graduate fellowship. PP acknowledges support from a Department of Science and Technology (DST)- Woman of Science (WOS-A) grant as well as past funding from Department of Biotechnology (DBT) Bio-CARe, Indian Institute of Science Education and Research (IISER) Mohali and an IA grant awarded to KB. KB was an Intermediate Fellow of the India Alliance (IA) and thanks the Alliance for funding support. KB also thanks DST- Science and Engineering Research Board (SERB) for funding support.

Funding

This work was supported by the Wellcome Trust/ DBT India Alliance Fellowship [grant number IA/I/12/1/500516] awarded to KB and partially supported by a DST– SERB grant [SERB/F/7047] to KB. PP is supported by a DST WOS-A grant [SR/WOS-A/LS-285/2018] and was earlier supported by a DBT Bio-CARe grant [BioCARe/01/10167]. AG-R lab is supported by the NBRC core fund from the Department of Biotechnology and Wellcome Trust-DBT India Alliance (Grant # IA/I/13/1/500874).

Author Contributions

PP and AS designed, performed, analyzed all the experiments and wrote the manuscript. PP and AS are co-first authors listed alphabetically. HK and AG-R helped with performing the ablation experiments and editing the manuscript. KB supervised the experiments, helped with experimental design and data interpretation and edited the manuscript.

.

The authors declare no conflict of interest.

Figure Legends

Fig. 1: Analysis of movement defects upon exposure to 400 mM ethanol. (a) *C. elegans* body-bends in the anterior and posterior regions marked by a partition. (b) Amplitude of body-bends shown by a double-sided arrow. (c) Quantitative analysis of WT *C. elegans* for number of body-bends in case of untreated (-EtOH) and 400 mM Ethanol exposed animals (+EtOH). Body-bends were counted for 1 minute (min) after 2 hours (h) in both sets of animals (+/-EtOH). The number of body-bends per minute in the anterior and posterior region of the animal were plotted with posterior body-bends shown in blue in all figures. Experiments were carried out in triplicates with 10 worms each. In this graph F = 20.9 and DF = 3. (d) Quantitative analysis of amplitude of body-bends for WT untreated (-EtOH) and WT worms exposed to 400 mM EtOH (+EtOH). The amplitude of body-bends was analyzed for the animals using ImageJ and the measure is represented in μm. The amplitude of body-bends in the anterior and posterior regions of the animal were plotted with posterior body-bends shown in blue in all figures. The experiments were performed in duplicates and 20 worms were quantitated and represented in graphs. The same animals were used to quantitate body-bends and amplitude of body-bends for all figures. In this graph F = 6.97 and DF = 3. (e) Quantitative analysis of number of body-bends for WT and *dop-2* mutant worms, both treated with EtOH (F = 299, DF = 3). (f) Quantitative analysis of amplitude of body-bends for WT and *dop-2* mutant animals, both treated with EtOH (+EtOH) (F = 96.6, DF = 3) (g) Comparison of number of body-bends for WT and *dop-2* mutants in the absence of EtOH (-EtOH), (F = 7.57, DF = 3). (h) Quantitative analysis of amplitude of body-bends for WT and *dop-2* mutant worms in the absence of EtOH (-EtOH), (F = 4.09, DF

= 3). Error bars represent ±S.E.M. and p-values were calculated using one-way ANOVA and Turkey-Kramer multiple comparison test; "***" indicates p<0.001 and "ns" indicates not significant in all graphs.

Fig. 2: DOP-2 functions in the PDE neuron for the Ethanol Induced Sedetive (EIS) behavior. (a) Graph indicating body-bend measurements for rescue of the *dop-2* behavior using transgenic expression of DOP-2 under the *dop-2* promoter, (F = 109, DF = 7). (b) Graph indicates amplitude of body-bend measurements for WT, *dop-2* and rescue lines (F =74.6, DF = 7). (c) Illustration of PDE neuron ablation. (d) Quantitation of the number of body-bends in mock ablated and PDE ablated animals, (F =140, DF = 7) (e) Quantitation of the amplitude of body-bends in mock ablated and PDE ablated *C. elegans,* (F = 48.8, DF = 7). All experiments in this figure were performed in the presence of EtOH (+EtOH). Error bars represent ±S.E.M. and p-values were calculated using one-way ANOVA and Turkey-Kramer multiple comparison test; "**" indicates p<0.01, "***" indicates p<0.001 and "ns" indicates not significant in all panels.

Fig. 3: Role of dopamine in the ethanol induced behavior. (a) Graph represents the number of body-bends in WT, *dop-2, cat-2 and cat-2; dop-2* mutants in the presence of EtOH, (F = 265, DF = 7). (b) Quantitation of the amplitude of body-bends in WT, *dop-2*, *cat-2 and cat-2; dop-2* strains in the presence of EtOH, (F = 44.1, DF = 7). (c) Graph representing the number of body-bends in WT animals under different conditions (+ EtOH, + DA and + DA + EtOH), (F = 169, DF = 5). (d) Graph shows the amplitude of body-bends in WT *C. elegans* under different conditions (+ EtOH, + DA, + DA + EtOH), (F = 107, DF = 5). Error bars represent ±S.E.M and p-values were calculated using one-way ANOVA and Turkey-Kramer multiple comparison test; "*" indicates p<0.05,

880 "**"indicates p<0.01, "***"indicates p<0.001 and "ns" indicates not significant in all
881 panels.

882 **Fig. 4: Mutants in *dop-2* show increased dopamine release in presence of ethanol.**
883 (a) Fluorescence recovery after photobleaching (FRAP) was performed on the PDE
884 neuron synapses labeled with P*asic-1*::SNB-1::SEpHluorin. Representative images
885 before bleaching (-10 seconds (sec)), followed by bleaching (0 sec) and post bleach at
886 60 sec and 120 sec. (b) Quantitation of rate of recovery in WT and *dop-2* mutant
887 backgrounds with and without (+/- EtOH) treatment over 120 sec FRAP time course.
888 Data represents 20-22 synapses per genotype. (c) Representative dot plots from FRAP
889 data for percentage recovery at 60 sec and 120 sec time points respectively. (d)
890 Representative images of DAT-1::GFP expression in WT and *dop-2* mutant background
891 with and without EtOH treatment. (e) Whole cell fluorescence quantification of DAT-
892 1::GFP in PDE neurons for WT and *dop-2* mutants with and without EtOH (n=20). Error
893 bars represent ±S.E.M., n represents the number of animals analyzed and p-values
894 were calculated using one-way ANOVA and Turkey-Kramer multiple comparison test; "*"
895 indicates p<0.05, "**"indicates p<0.01, "***" indicates p<0.001 and "ns" indicates not
896 significant in all panels.

897 **Fig. 5: DOP-2 functions through the DOP-1 in the DVA neuron.** (a) Graph shows
898 number of body-bends in WT, *dop-2*, *dop-1*, *dop-2; dop-1* double mutants and the *dop-1*
899 rescue line (*dop-2; dop-1*; P*DVA*::DOP-1) on EtOH treatment; (F = 212, DF = 9). (b)
900 Graph shows amplitude of body-bends in WT, *dop-2*, *dop-1*, *dop-2; dop-1* double
901 mutant and the *dop-1* rescue line (*dop-2; dop-1*; P*DVA*::DOP-1) on EtOH treatment, (F
902 = 105, DF = 9). (c) Quantitation of number of body-bends in WT, *dop-2* and three NLP-

12 overexpression lines upon EtOH treatment, (F = 302, DF = 9). (d) Quantitation of amplitude of body-bends in WT, *dop-2* and three NLP-12 overexpression lines upon EtOH treatment, (F = 77.2, DF = 9). Error bars represent ±S.E.M. and p-values were calculated using one-way ANOVA and Turkey-Kramer multiple comparison test; "*" indicates $p<0.05$, "**" indicates $p<0.01$, "***" indicates $p<0.001$ and "ns" indicates not significant in all panels.

Fig. 6: Increased acetylcholine signaling causes increased sensitivity to ethanol in WT animals. (a) Graph of number of body-bends for WT and *cha-1* mutants on EtOH plates after treatment with aldicarb, (F = 254, DF = 5). (b) Graph indicates amplitude of body-bends for WT and *cha-1* mutants on EtOH plates after treatment with aldicarb, (F = 68.6, DF = 5). (c) Quantitation of number of body-bends from WT, *acr-16* and the ACR-16++ line on EtOH, (F = 28.2, DF = 5). (d) Quantitation of amplitude of body-bends from WT, *acr-16* and the ACR-16++ line on EtOH, (F = 18.4, DF = 5). Error bars represent ±S.E.M. and p-values were calculated using one-way ANOVA and Turkey-Kramer multiple comparison test; "*" indicates $p<0.05$, "**" indicates $p<0.01$, "***" indicates $p<0.001$ and "ns" indicates not significant in all panels.

Fig. 7: Proposed model for DOP-2 functioning in the presence of EtOH. (a) DOP-2 DA autoreceptors functions in the posterior DA neurons (PDE) to regulate DA levels, in the presence of EtOH. (b) Loss of the *dop-2* autoreceptor leads to unregulated release of DA in the presence of EtOH. The increased levels of DA activate the function of DOP-1 receptors present on the DVA neuron causing increased DVA activation. This in turn causes increased release of the neuropeptide NLP-12, which in turn could cause

925 increased cholinergic signaling at the NMJ. This model is based on this work and prior
926 studies (Bhattacharya et al., 2014; Hu et al., 2011).

927

928 **Fig. S1: Ethanol dependent phenotype of dopaminergic pathway mutants**. (a)
929 Graph of number of body-bends (posterior body-bends are shown in blue) in WT, *cat-2*,
930 *dat-1*, *dop-1*, *dop-2*, *dop-3* and *slo-1* mutants upon EtOH treatment. Experiments were
931 performed in triplicates with 10 worms per assay in all the figures. For this graph F =
932 66.8 and DF = 13. (b) Graph of amplitude of body-bends (posterior body-bends are
933 shown in blue) for WT, *cat-2*, *dat-1*, *dop-1*, *dop-2*, *dop-3* and *slo-1* mutants upon EtOH
934 treatment. Ten animals were used for each experiment to quantitate the amplitude of
935 body-bends and the experiment was performed in duplicate for all figures. The same
936 videos of moving animals were used to quantitate both number and amplitude of body-
937 bends. For this graph F = 306 and DF = 13. In both graphs mutants in the EtOH sensing
938 channel protein, *slo-1* were used as positive control. Error bars represent ±S.E.M. and
939 p-values were calculated using one-way ANOVA and Turkey-Kramer multiple
940 comparison test; "*" indicates $p<0.05$, "**" indicates $p<0.01$, "***" indicates $p<0.001$ and
941 "ns" indicates not significant in all panels.

942 **Fig. S2: Mutants in *dop-2* do not show defects in pharyngeal pumping.** The graph
943 shows the quantitation of the number of pharyngeal pumps in 1 min from WT, *dop-2* and
944 *slo-1* mutants in the presence of EtOH. The experiment was performed with 10 animals
945 per experiment in duplicate. Error bars represent ±S.E.M. and p-values were calculated
946 using one-way ANOVA and Turkey-Kramer multiple comparison test; "***" indicates
947 $p<0.001$ and "ns" indicates not significant.

948 **Fig. S3: Diagrammatic representation of the FRAP experiment.** A pH sensitive GFP
949 Fluorophore, pHluorin, was tagged to the synaptic vesicle protein SNB-1 and expressed
950 in DA neurons. This line was constructed and previously used (Hardaway et al., 2015).

951 **Fig. S4: DVA ablation affects locomotion in WT animals.** (a) Quantitation of the
952 number of body-bends from WT and *nlp-12* mutant animals upon EtOH treatment, (F =
953 12.2, DF = 3). (b) Quantitation of the amplitude of body-bends from WT and *nlp-12*
954 mutants upon EtOH treatment, (F = 10.1, DF = 3). (c) Graph represents number of
955 body-bends in mock and DVA ablated WT animals, 10 animals were used for the mock
956 treatment and 11 for the DVA ablation. The experiment was performed in triplicate, (F =
957 368, DF = 3). (d) Graph shows the amplitude of body-bends in mock and DVA ablated
958 WT animals, 10 animals were used for the mock treatment and 11 for the DVA ablation.
959 The experiment was performed in duplicate (F = 197, DF = 3). Error bars represent
960 ±S.E.M. and p-values were calculated using one-way ANOVA and Turkey-Kramer
961 multiple comparison test; "***" indicates p<0.001 and "ns" indicates not significant.

962 **Fig. S5: Mutants in the cholinergic pathway do not show a phenotype in the**
963 **presence of EtOH.** (a) Graph indicates the number of body-bends quantitated from WT,
964 *cha-1* and *acr-16* mutants upon EtOH treatment, (F = 15, DF = 5). (b) Graph shows
965 amplitude of body-bends quantitated from WT, *cha-1* and *acr-16* mutants upon EtOH
966 treatment, (F = 10.8, DF = 5). Error bars represent ±S.E.M. and p-values were
967 calculated using one-way ANOVA and Turkey-Kramer multiple comparison test; "ns"
968 indicates not significant in both panels.
969

Fig. 1

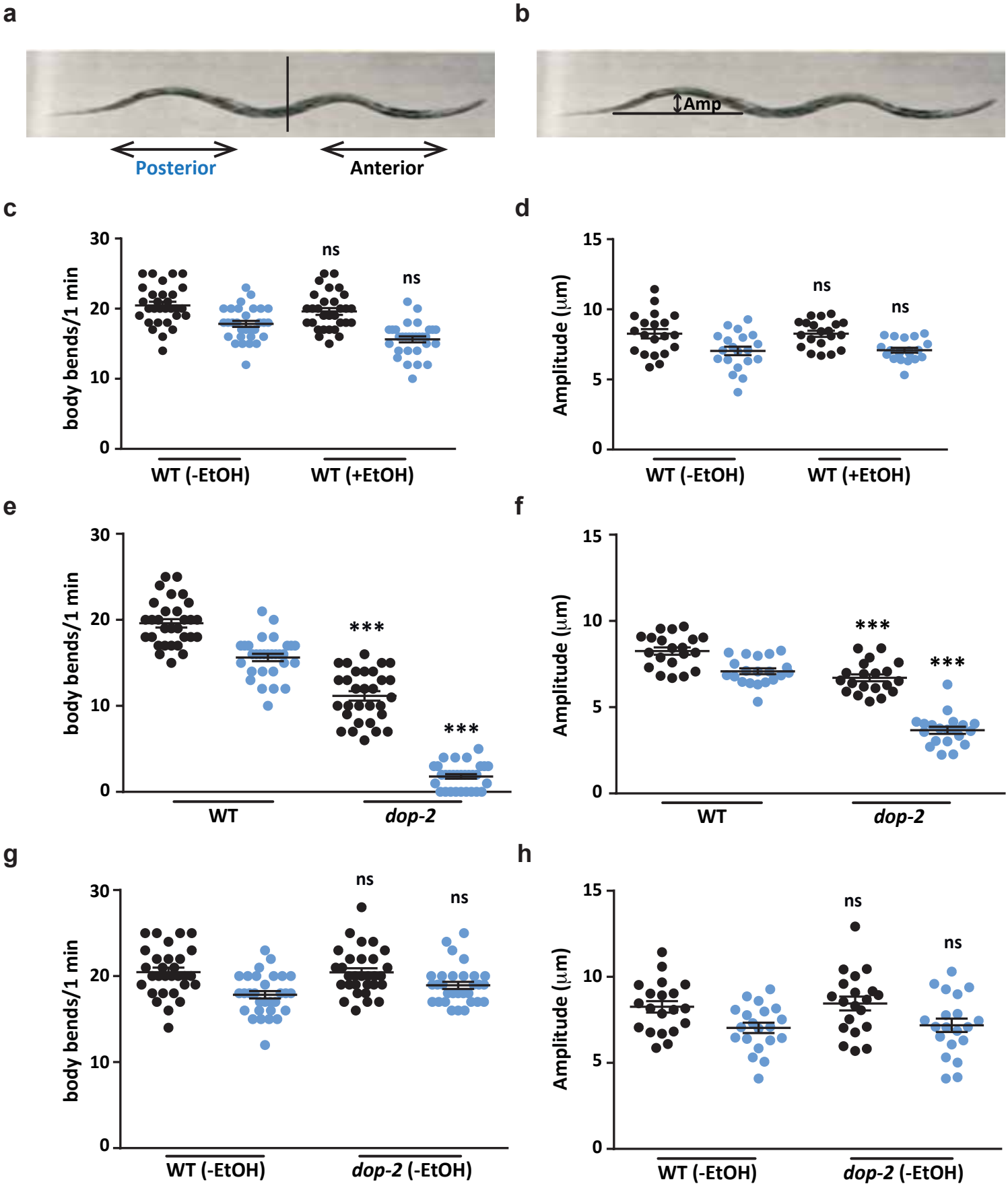

Fig. 2

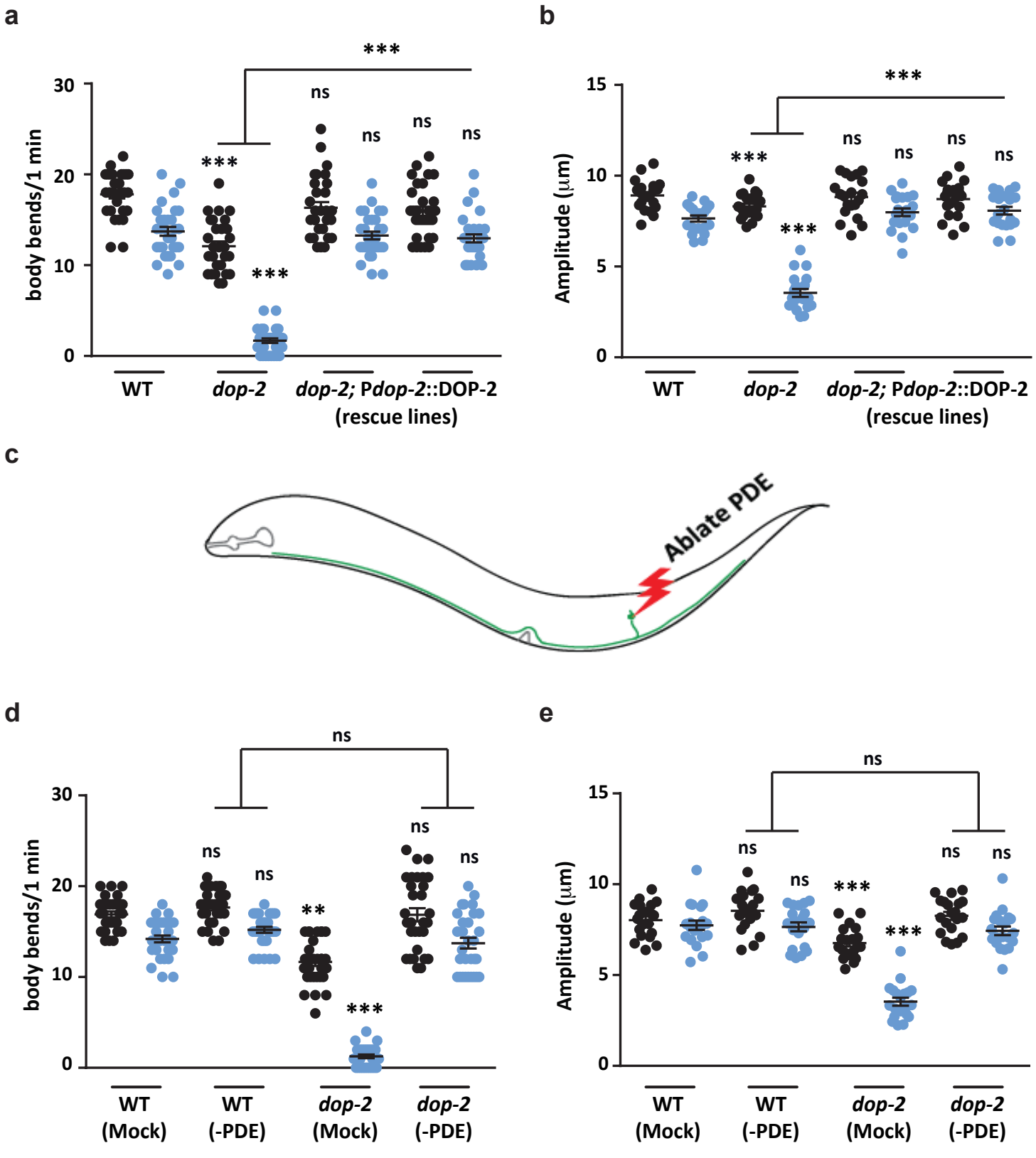

Fig. 3

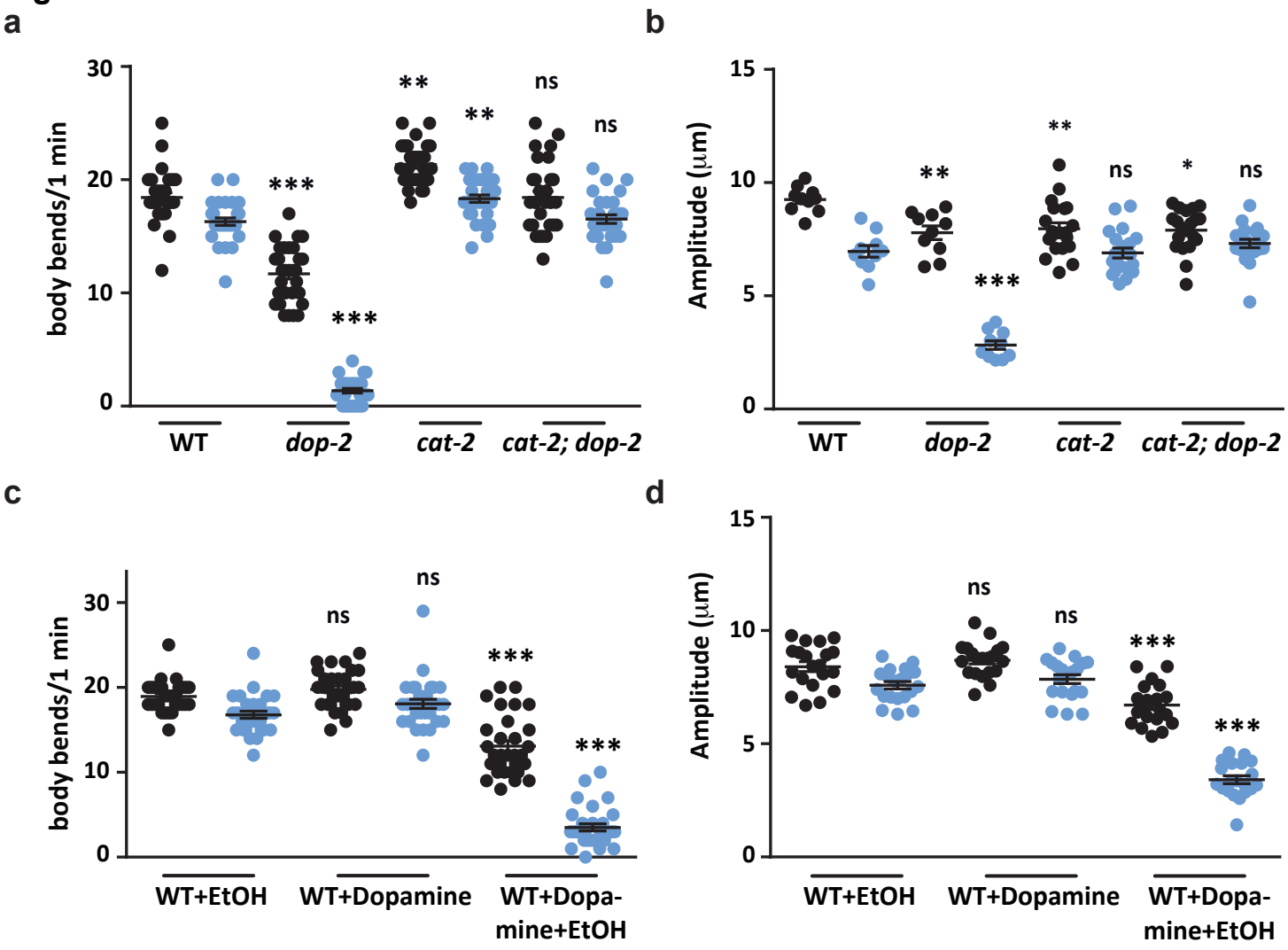

Fig. 4

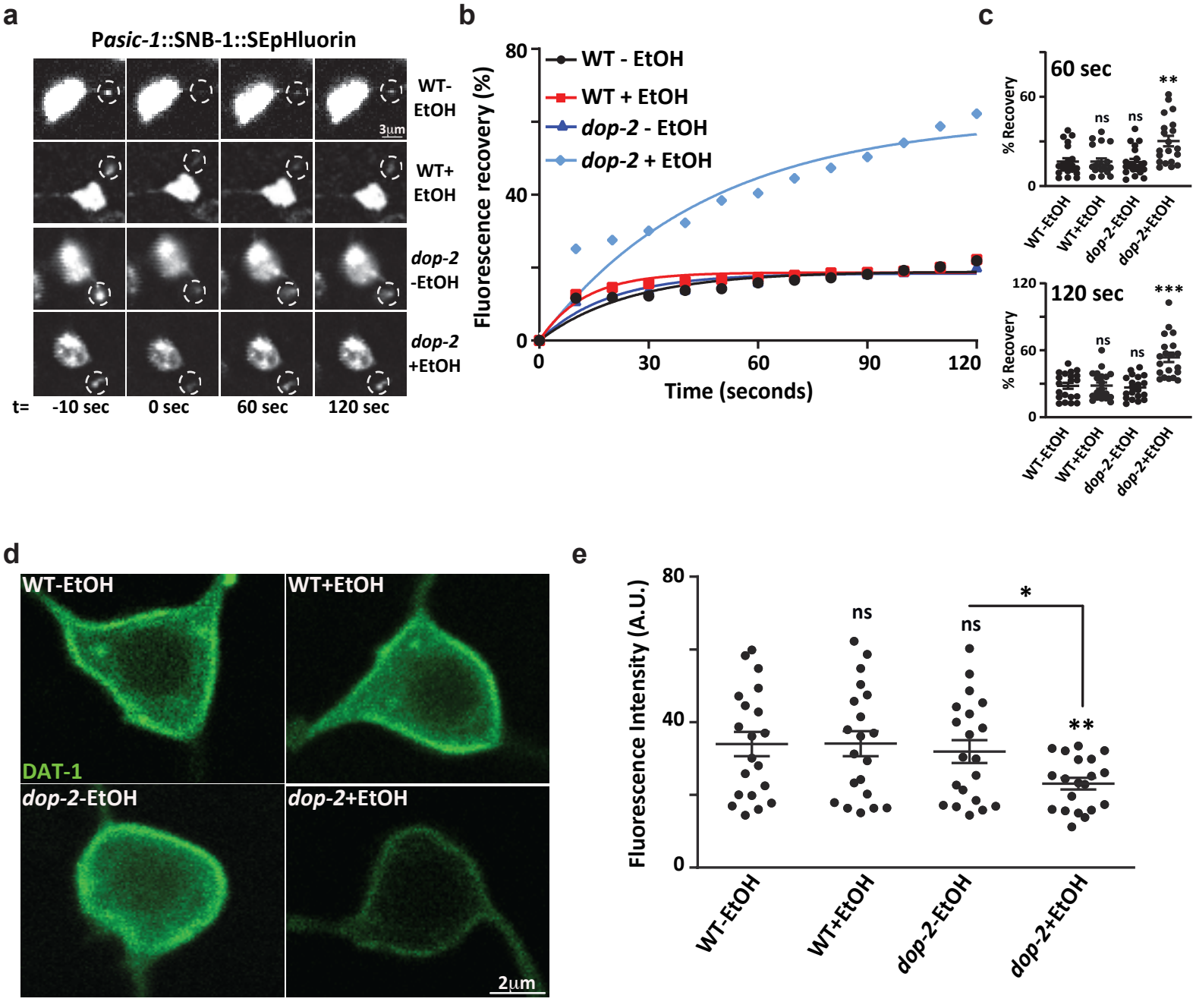

Fig. 5

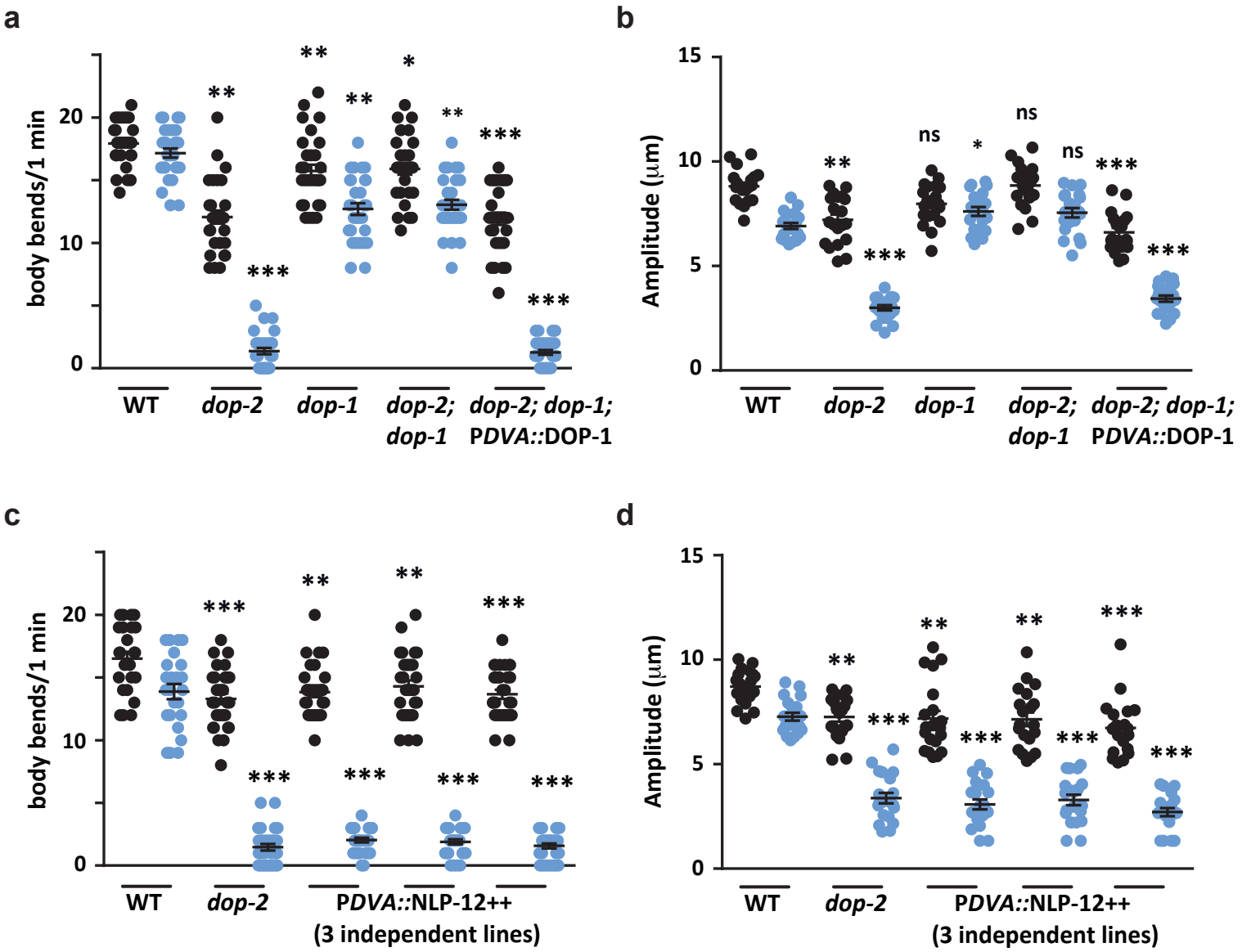

Fig. 6

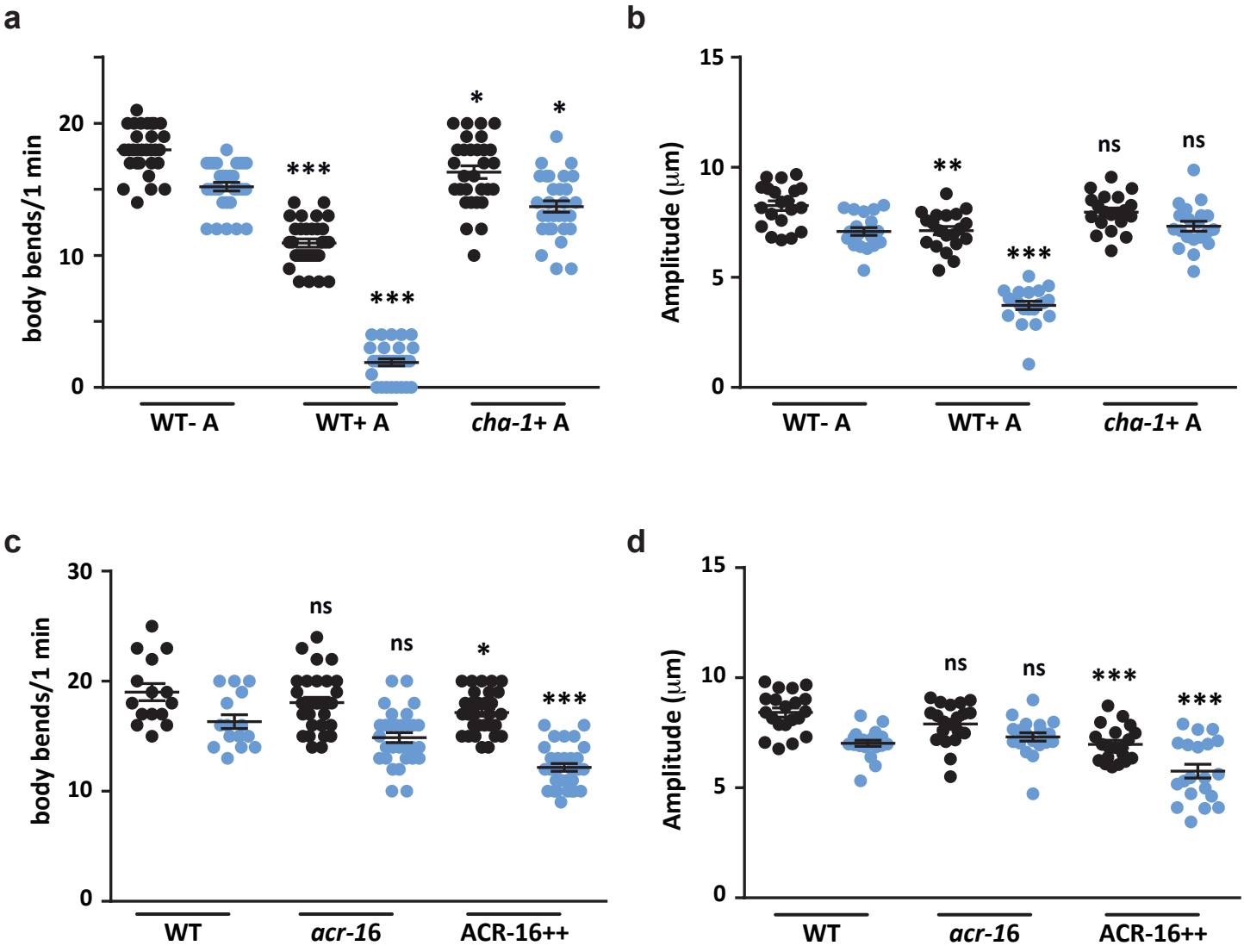

Fig. 7

a

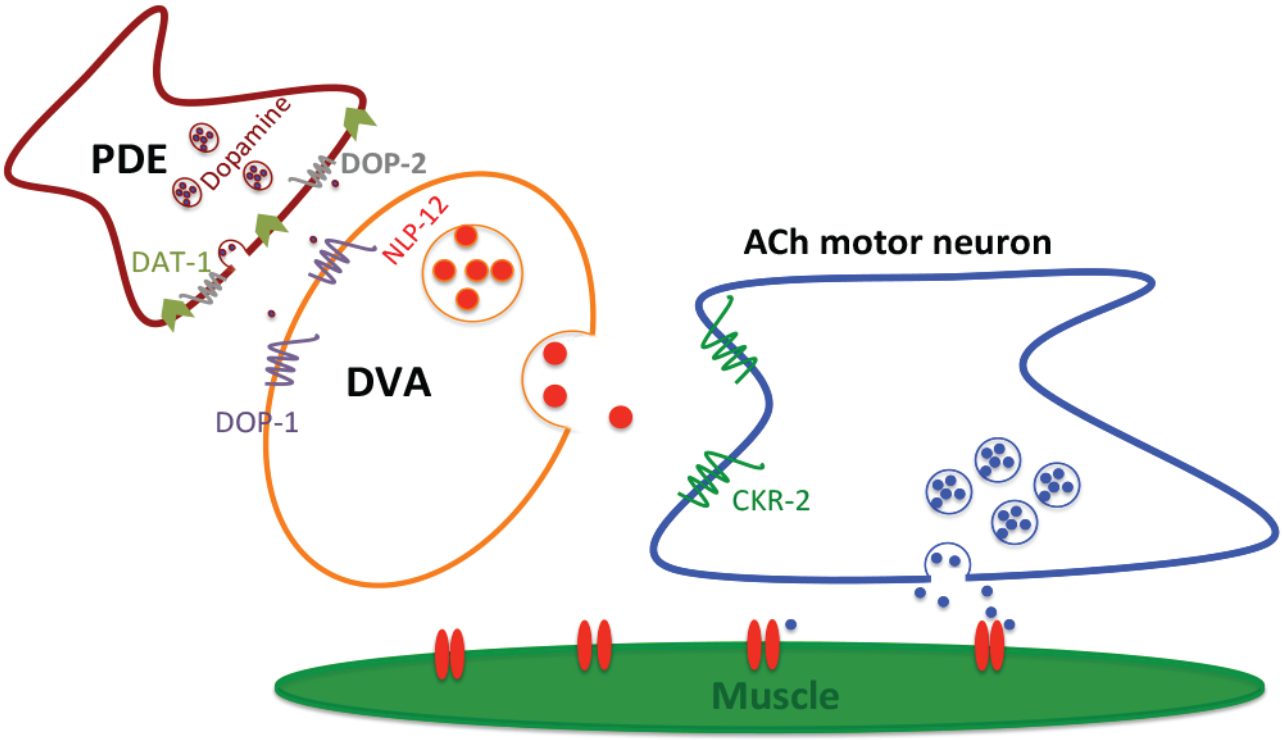

b

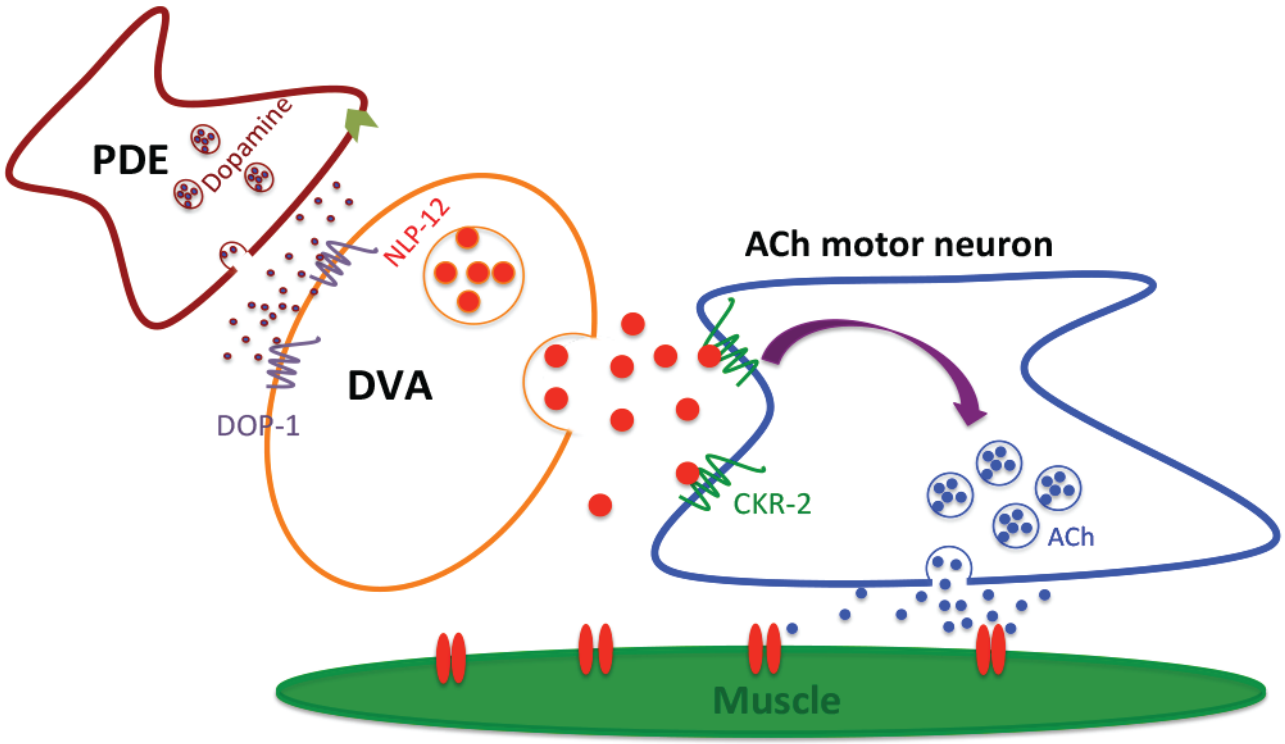

Supplementary Figure 1

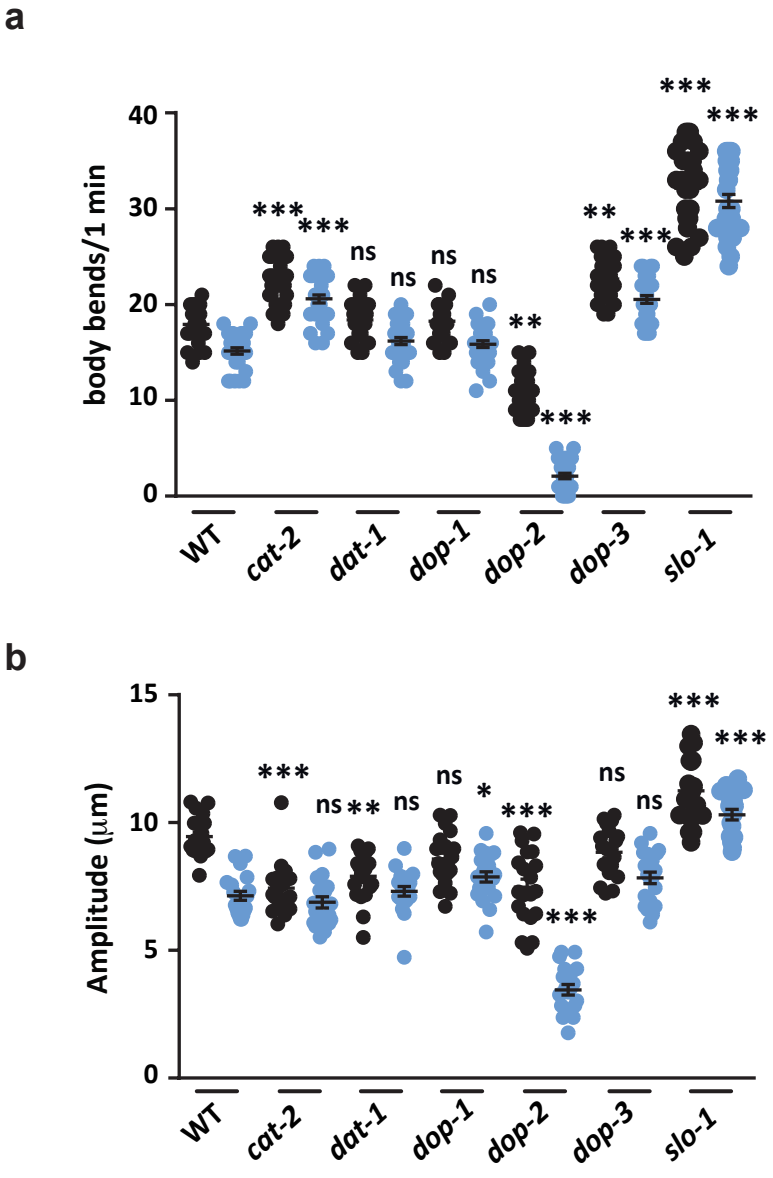

Supplementary Figure 2

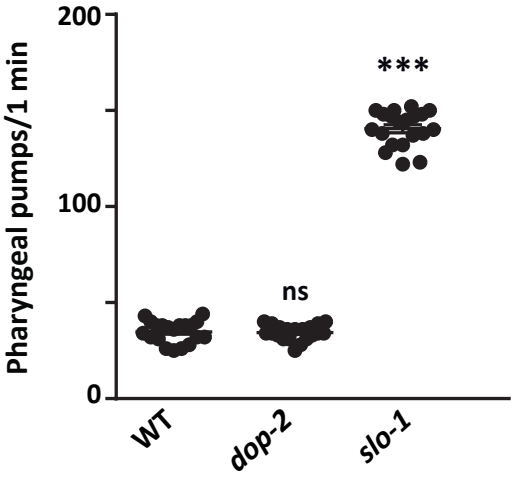

Supplementary Figure 3

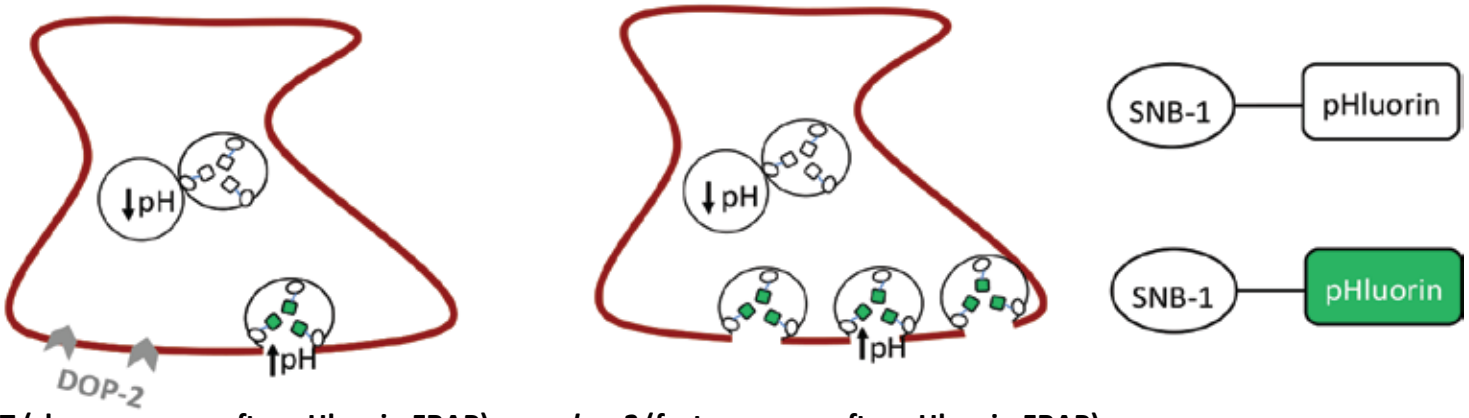

WT (slow recovery after pHluorin FRAP) **_dop-2_ (fast recovery after pHluorin FRAP)**

Supplementary Figure 4

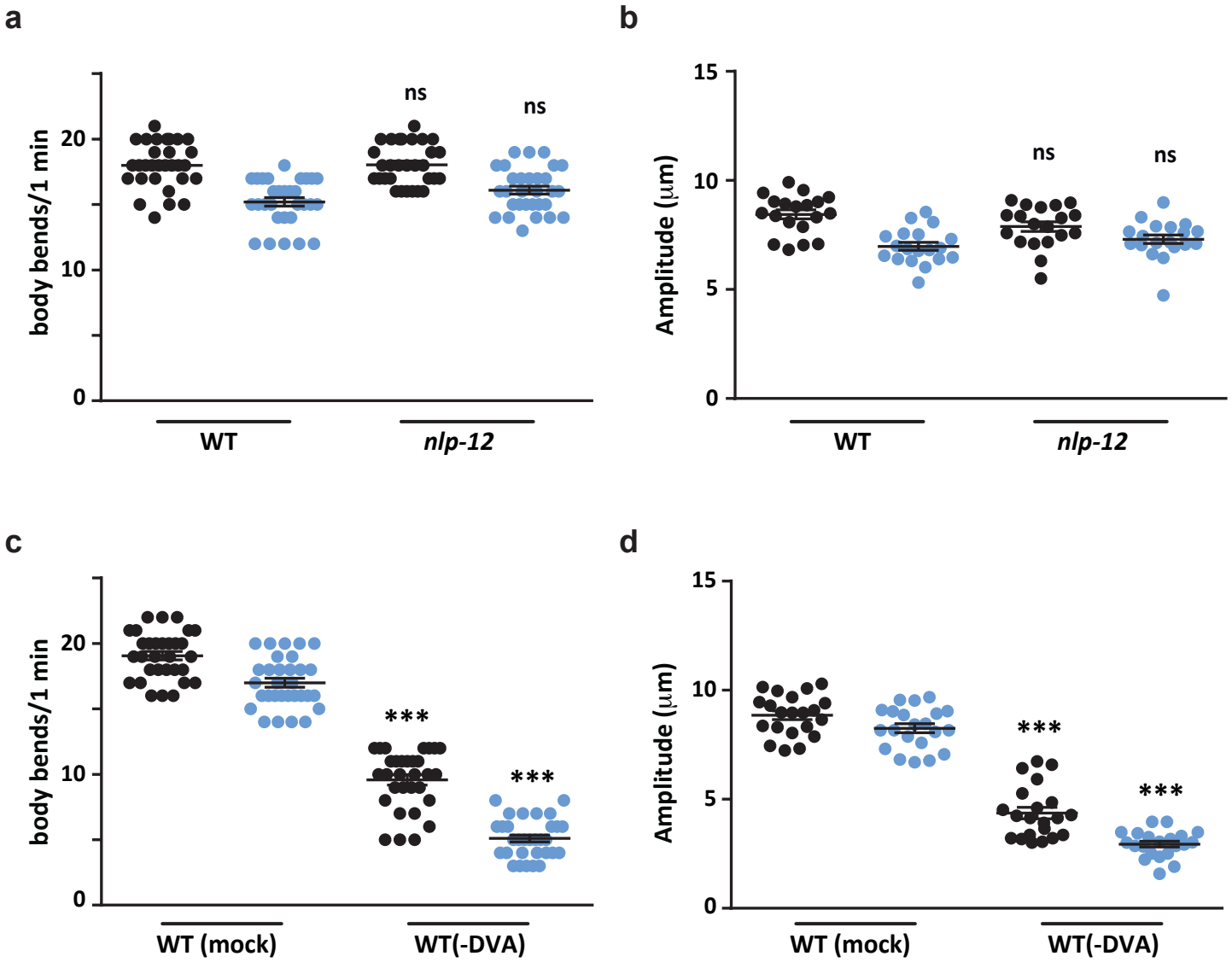

Supplementary Figure 5

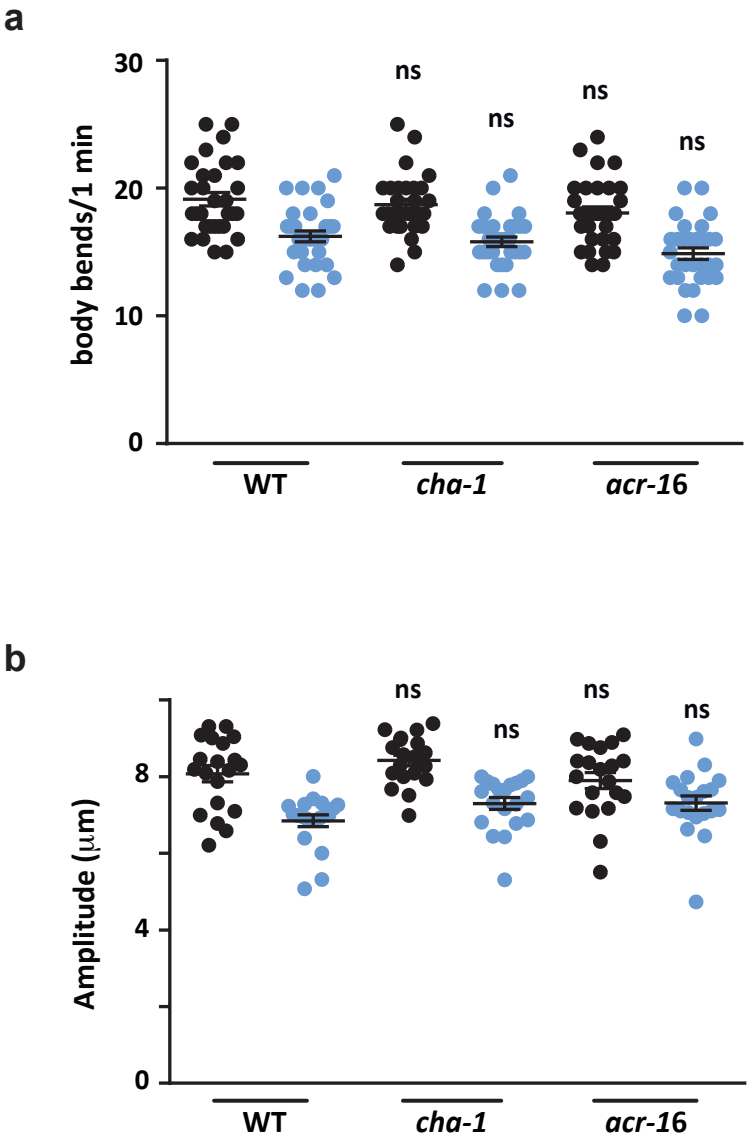

Supplementary tables

Table S1: List of strains used in this study

Strain	Genotype	Comments
LX702	*dop-2(vs105)V*	CGC strain
LX703	*dop-3(vs106)X*	CGC strain
LX645	*dop-1(vs100)X*	CGC strain
MT15620	*cat-2(n4547)II*	CGC strain
PR1152	*cha-1(p1152)IV*	CGC strain
RB918	*acr-16(ok789)V*	CGC strain
BZ142	*slo-1(eg142)V*	CGC strain
RM2702	*dat-1(ok157)III*	CGC strain
RB607	*nlp-12(ok335)*	CGC strain
nuIs299	P*myo-3*::ACR-16::GFP	Josh Kaplan Lab
IR724	*asic-1*::*SNB-1*::SEpHlourin	Blakely Lab
BY834	P*dat-1*::DAT-1::GFP	Blakely Lab
BZ555	egIs1(P*dat-1*::gfp)	CGC strain
BAB900	*dop-1(vs100); dop-2(vs105)*	This study
BAB901	*cat-2(n4547); dop-2(vs105)*	This study
BAB902	*egIs1*(Pdat-1::gfp); *dop-2(vs105)*	This study
BAB903	P*dat-1*::DAT-1::GFP; *dop-2(vs105)*	This study
BAB904	*asic-1*::*SNB-1*::SEpHlourin; *dop-2(vs105)*	This study
BAB905	P*dop-2*::DOP-2::CFP;*dop-2* (IndEx905)	This study
BAB906	P*nlp-12*::NLP-12 (IndEx906)	This study
BAB907	P*nlp-12*::DOP-1::*wrm* Scarlet; *dop-1(vs100);*	This study

	dop-2(vs105) (IndEx907)	
BAB908	P*nlp-12*::DOP-1::*wrm* Scarlet; *dop-1(vs100)* (IndEx908)	This study

Table S2: List of primers used in this study

Primer Code	Sequence	Comment	Gene
PRS37	CCCTTGAATGGCCTCCACC	Genotyping Forward External	*dop-2*
PRS38	CAGTACTCCGGTACCGAGCAC	Genotyping Forward Internal	*dop-2*
PRS39	CTCGGGAGCACTTGTGAGAG	Genotyping Reverse External	*dop-2*
PRS23	TCACAGATGTCCGTTTTCCA	Genotyping Forward External	*acr-16*
PRS24	TCAATGATTCCGAGTGACGA	Genotyping Reverse External	*acr-16*
PRS 314	GTGCCTGGAGGAGCGCAAATATTGG	Genotyping WT Forward	*slo-1*
PRS 315	GTGCCTGGAGGAGCGCAAATATTAA	Genotyping Mutant Forward	*slo-1*
PRS 316	GGACTTGCCCTGCGGTCCCGAATAC	Genotyping Reverse	*slo-1*
PRS 322	CCAAATTAGTCGAAAAGCTGATCCCGC	Genotyping Forward External	*dat-1*
PRS 323	GTGATCCTTGCCTGGGGGCTTC	Genotyping Forward Internal	*dat-1*
PRS 324	GAAGCCCCCAGGCAAGGATCAC	Genotyping Reverse External	*dat-1*
PRS 332	GGAATAGGAACCATAGAAGATCTCC	Genotyping Forward External	*cat-2*
PRS 333	CGATGACTGTGACACCGCGAGG	Genotyping Reverse External	*cat-2*
PRS 334	GGCCGAGAACTGATAACCCAGC	Genotyping Reverse Internal	*cat-2*

PRS 340	GGACCCAAACATGCCACAGTGATATGG	Genotyping Forward External	*dop-1*
PRS 341	GAAGATTCAGGCGAGTTGCATTCGC	Genotyping Reverse External	*dop-1*
PRS 342	GAATGCTCGTCTAAAGTCACGATTG	Genotyping Forward Internal	*dop-1*
PRS 343	GGTGTTCGCAATATTTGCGAAGACG	Genotyping Forward External	*dop-3*
PRS 344	CCATCAGCGTGCTTTACTCGTTCAC	Genotyping Reverse External	*dop-3*
PRS 345	GTGACGGTTTGTAGAGATCGTTCTC	Genotyping Forward Internal	*dop-3*
PRS 473	CCCCCCGGGATGAACGATTTGCAATGGCC	Cloning Forward XmaI	*dop-1* cDNA
PRS 474	CCCCCCGGGCTATTCCGGAATGGTTTCCTCG	Cloning Reverse KpnI	*dop-1* cDNA
AS1	AACTGCAGGGCCGAGACGAATCCGGAGG	Cloning Forward PstI	P*nlp-12*
AS4	CGGGATCCGCATTTTGTCGGAGGCAATTG	Cloning Reverse BamHI	P*nlp-12*
AS3	CGGGATCCGAAAATGTGTCGCTTCGAGAC	Cloning Reverse BamHI	NLP-12

Table S3: List of plasmids used in this study

S. No.	Plasmid No.	Plasmid	Source
1	pBAB911	P*dop-2*::DOP-2::CFP	Rene Garcia Lab
2	pBAB912	P*nlp-12*::GFP	This Study
3	pBAB913	P*nlp-12*::NLP-12	This Study
4	pBAB914	P*nlp-12*::*sl2*::*wrm* Scarlet	This Study
5	pBAB915	*Pnlp-12*::DOP-1:: sl2::*wrm* Scarlet	This Study